On Thinning Ice:
Modeling Sea Ice in a Warming Climate

Kenneth M. Golden
Department of Mathematics, University of Utah

What can math tell us about disappearing polar sea ice and its ecosystems?
What can sea ice tell us about modeling composite materials and multiscale systems?

Worby

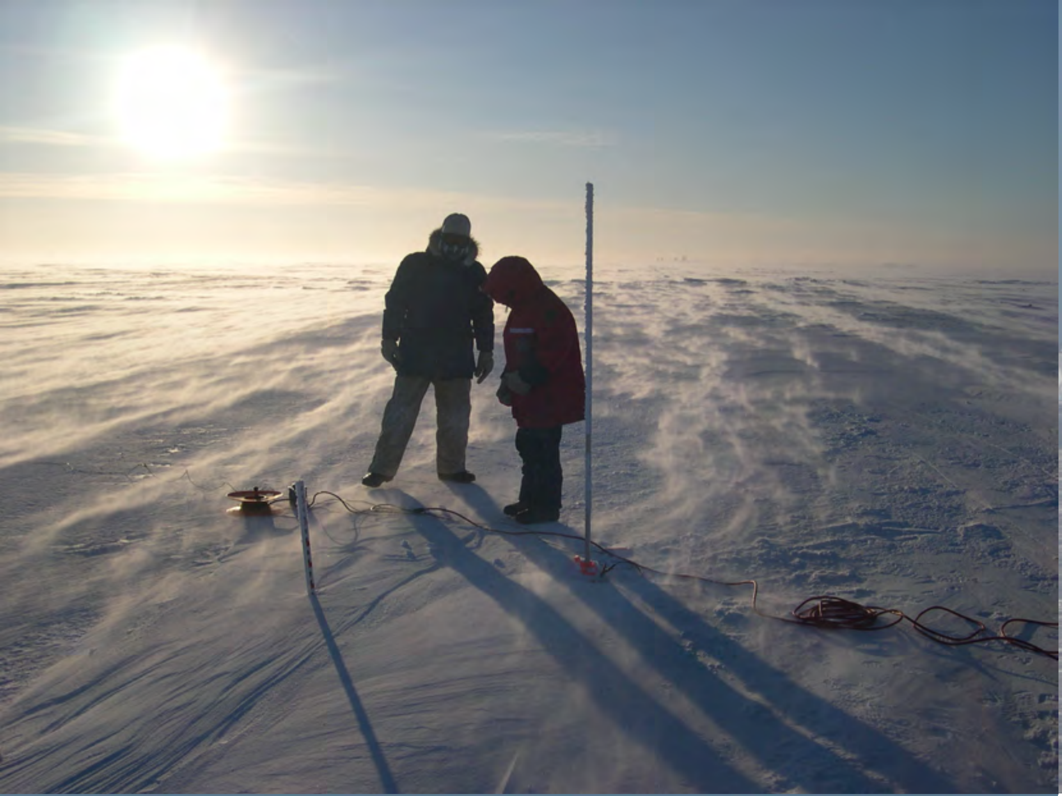

sea ice may appear to be a barren, impermeable cap ...

brine inclusions in sea ice (mm)

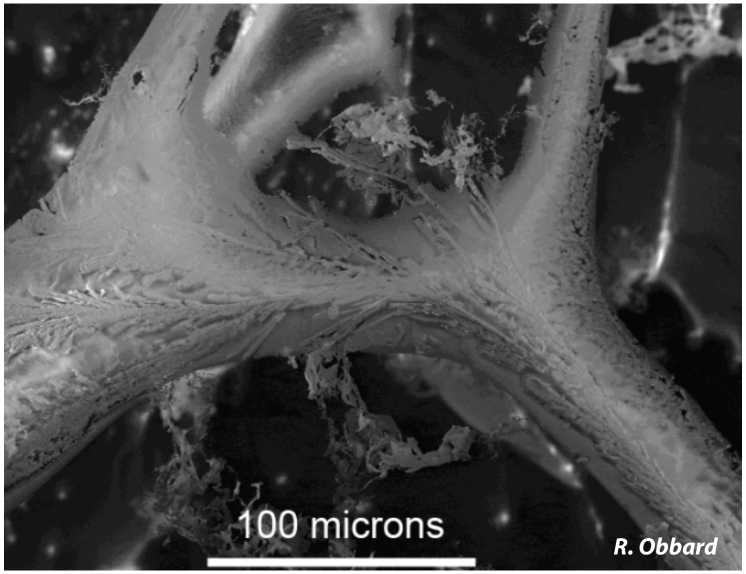

micro - brine channel (SEM)

brine channels (cm)

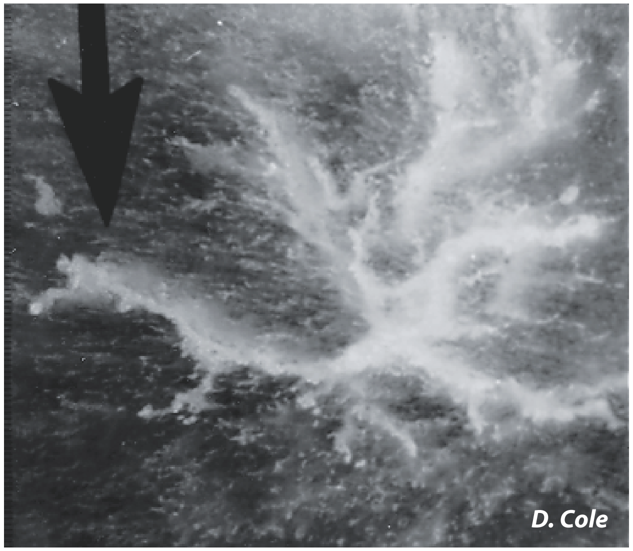

horizontal section

vertical section

sea ice is a porous composite

pure ice with brine, air, and salt inclusions

fluid flow through the porous microstructure of sea ice governs key processes in polar climate and ecosystems

evolution of Arctic melt ponds and sea ice albedo

nutrient flux for algal communities

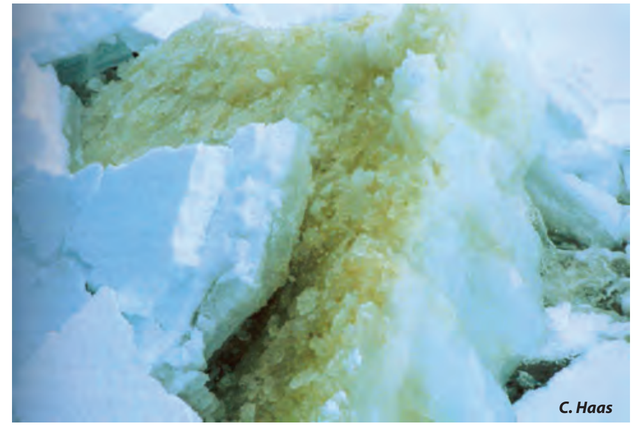

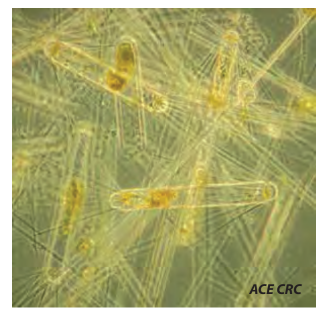

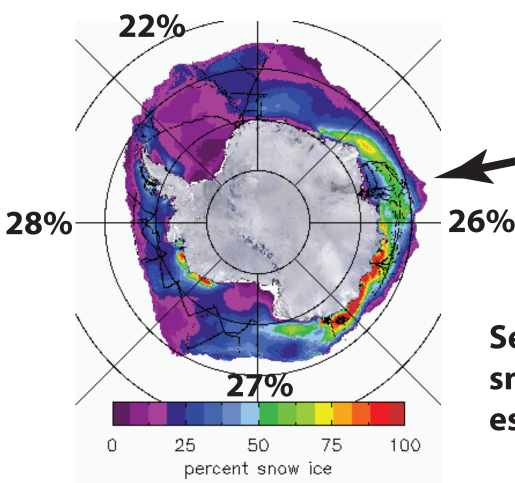

T. Maksym and T. Markus, 2008

September snow-ice estimates

Antarctic surface flooding and snow-ice formation

- *evolution of salinity profiles*
- *ocean-ice-air exchanges of heat, CO_2*

Arctic sea ice extent September 15, 2020

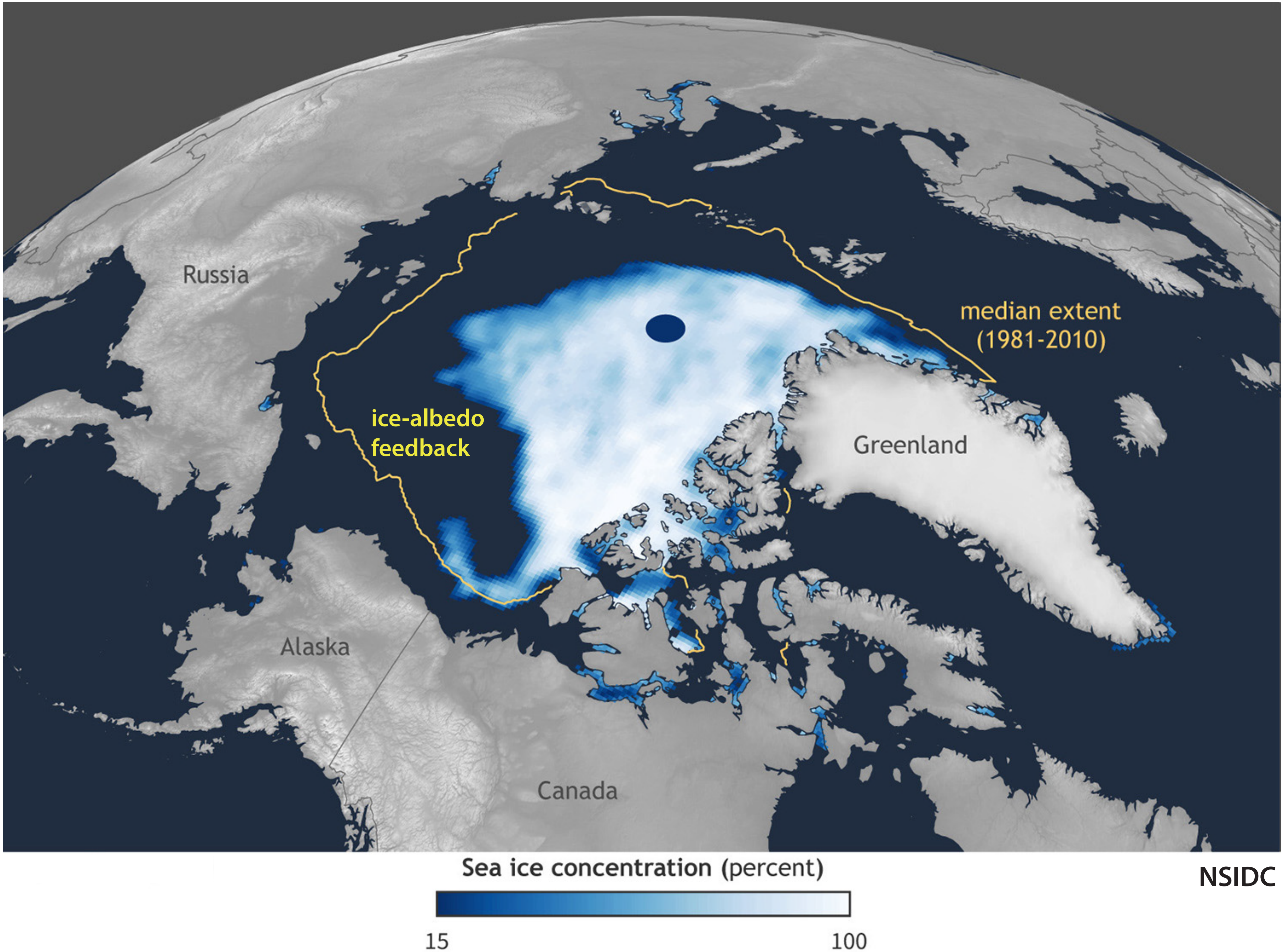

Predicting what may come next requires lots of math modeling.

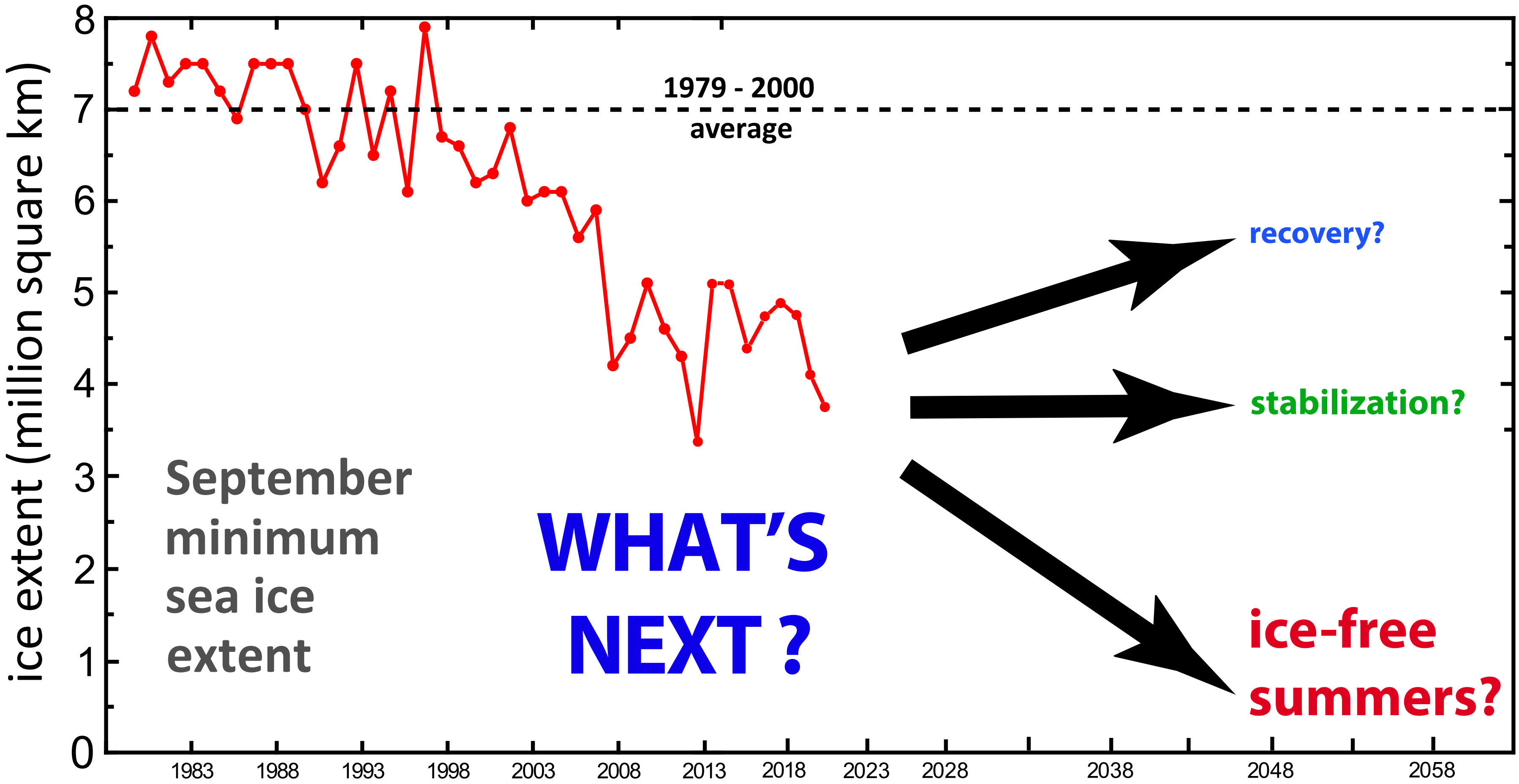

National Snow and Ice Data Center (NSIDC)

Sea Ice is a Multiscale Composite Material

microscale

brine inclusions

Weeks & Assur 1969

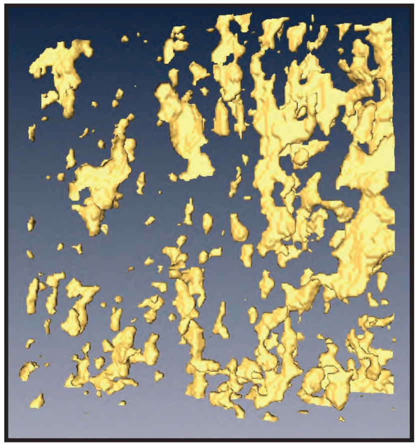

H. Eicken

Golden *et al. GRL* 2007

polycrystals

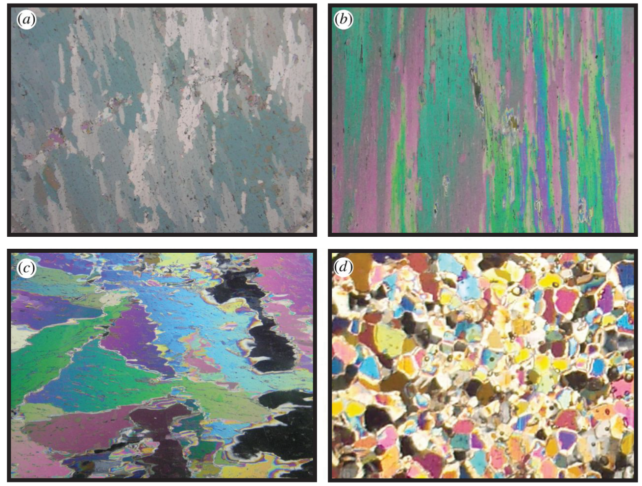

Gully *et al. Proc. Roy. Soc. A* 2015

brine channels

D. Cole

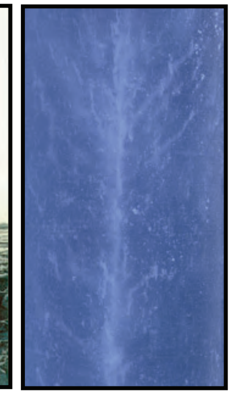

K. Golden

millimeters

centimeters

---

mesoscale

Arctic melt ponds

K. Frey

Antarctic pressure ridges

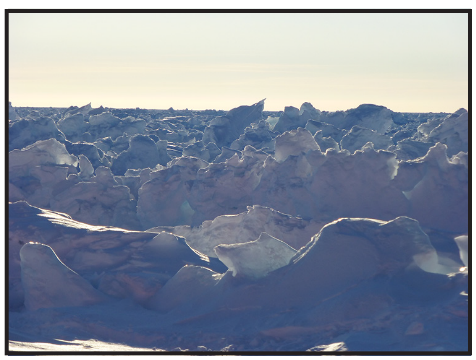

K. Golden

macroscale

sea ice floes

J. Weller

sea ice pack

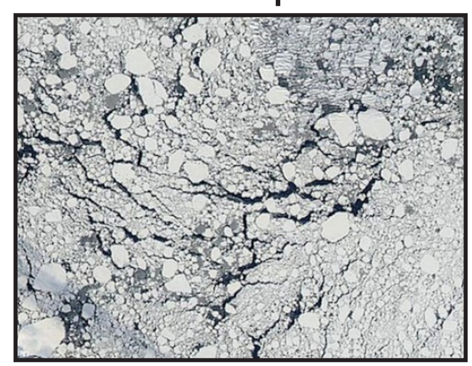

NASA

meters

kilometers

HOMOGENIZATION for Composite Materials

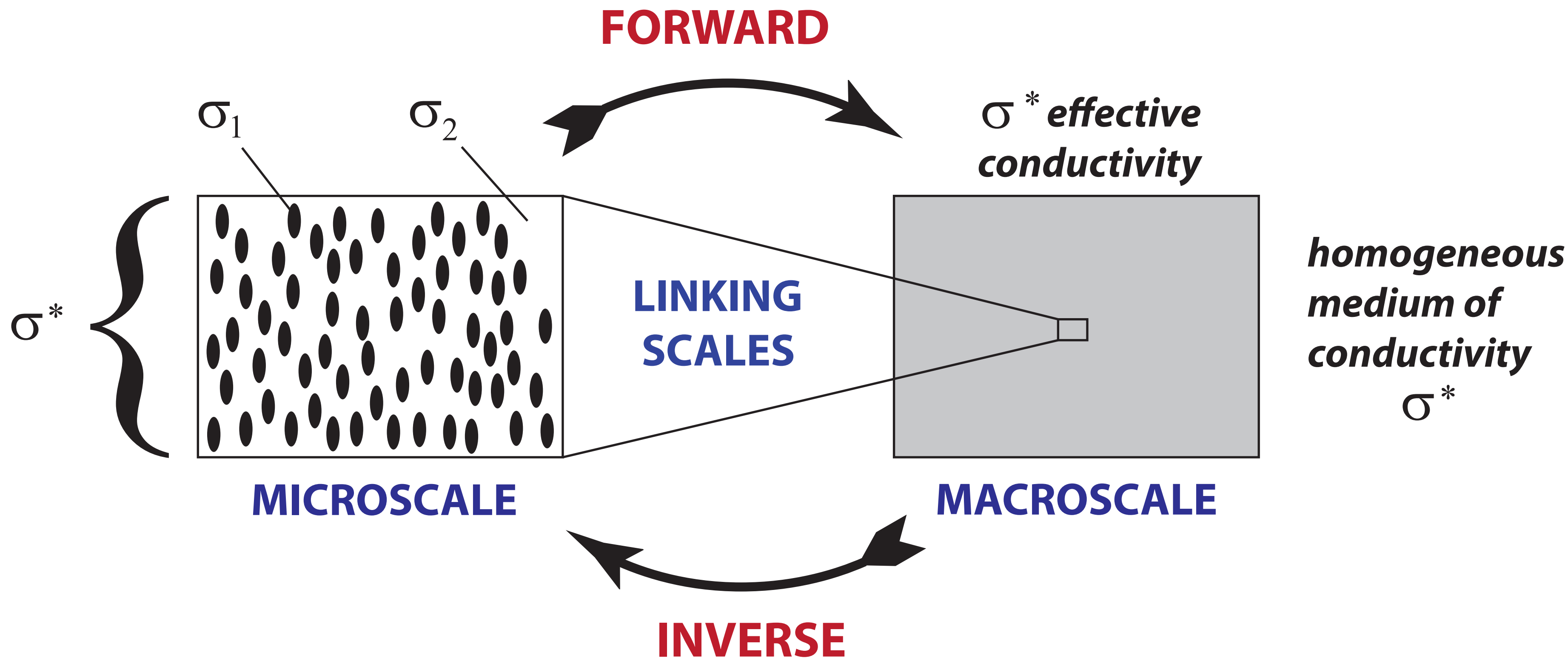

Maxwell 1873 : effective conductivity of a dilute suspension of spheres
Einstein 1906 : effective viscosity of a dilute suspension of rigid spheres in a fluid

*Wiener 1912 : arithmetic and harmonic mean **bounds** on effective conductivity*
*Hashin and Shtrikman 1962 : variational **bounds** on effective conductivity*

widespread use of composites in late 20th century due in large part to advances in mathematically predicting their effective properties

What is our research about?

- **Developing mathematical models of sea ice and its role in the climate system and polar ecosystem.**

Rigorously compute effective or collective behavior
multiscale homogenization
Improve climate models and projections of polar
sea ice and the ecosystems they support

physics of climate

sea ice

polar marine ecosystems

- **Solving problems in sea ice physics drives advances in composite materials, transport phenomena, porous media, inverse problems, biophysics.**

Polar Ecology and and the Physics of Sea Ice

Golden

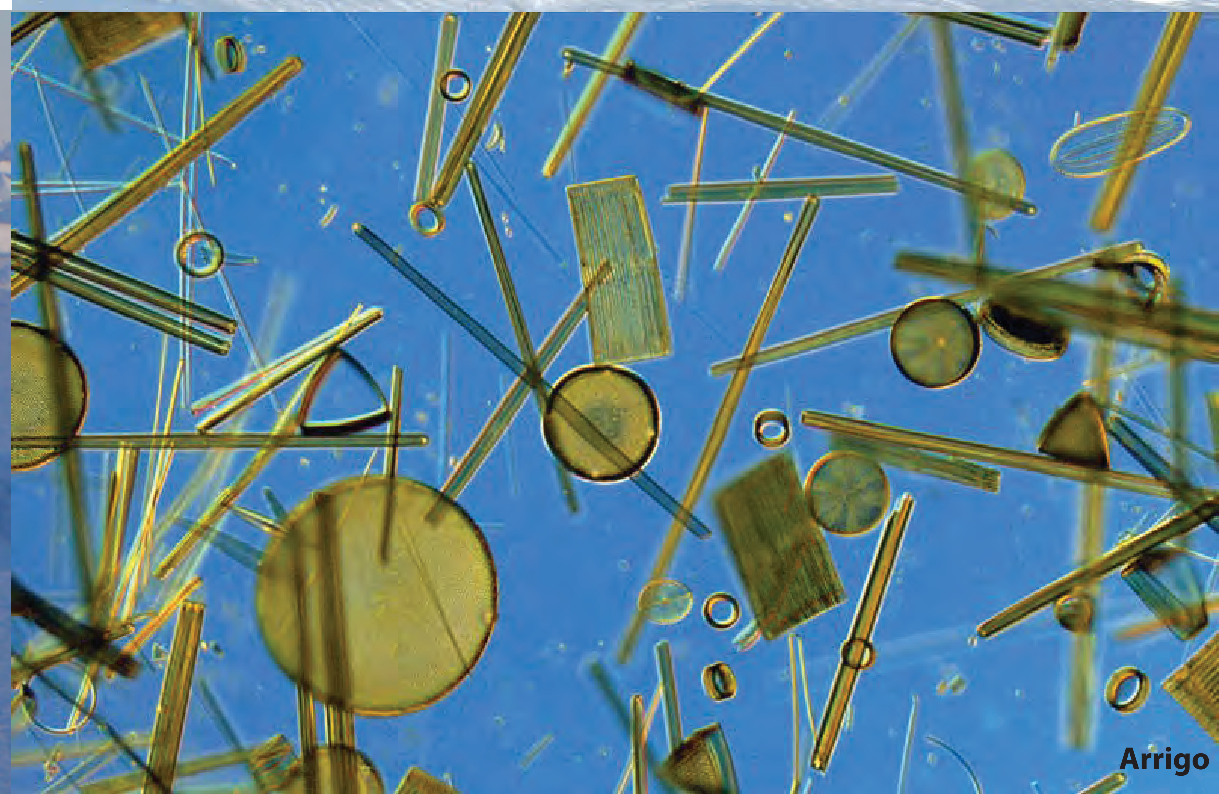

Arrigo

What kind of math do we use?

Whatever we need to answer big scientific questions, which often leads to new math!

partial differential equations (Laplace, heat, wave)

stochastic processes, advection diffusion, fractional diffusion

homogenization, percolation theory

statistical mechanics, solid state physics

dynamical systems and bifurcation theory

functional analysis, complex analysis, spectral theory

random matrix theory

inverse problems

machine learning, “hidden physics”, neural nets

uncertainty quantification, polynomial chaos

Morse theory, topology of surfaces, persistent homology

What is this talk about?

Using methods of **homogenization and statistical physics** to model sea ice effective behavior and advance representation of sea ice in climate models, process studies, ...

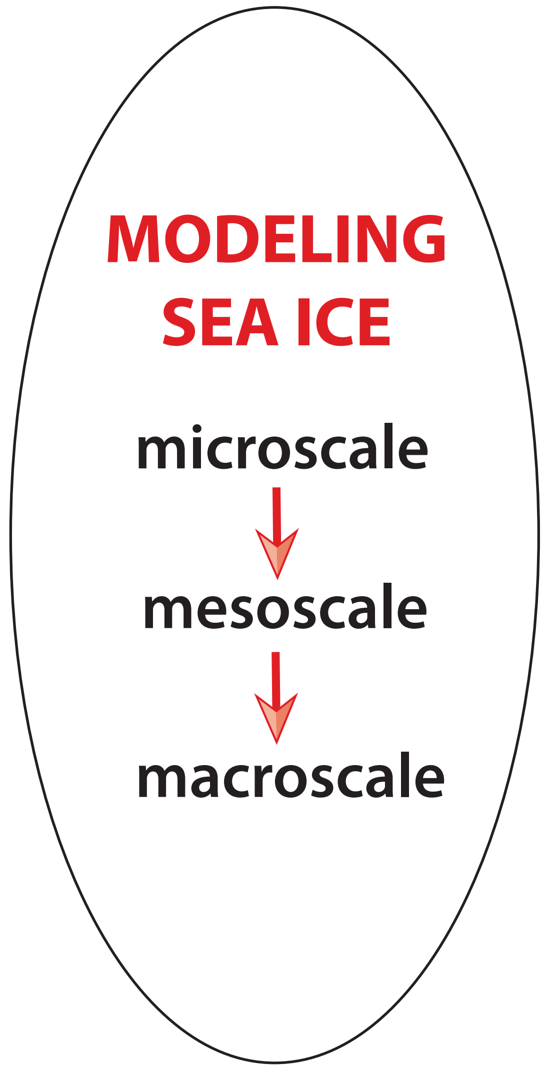

A tour of key sea ice processes on micro, meso, and macro scales.

microscale

brine volume fraction and ***connectivity*** increase with temperature

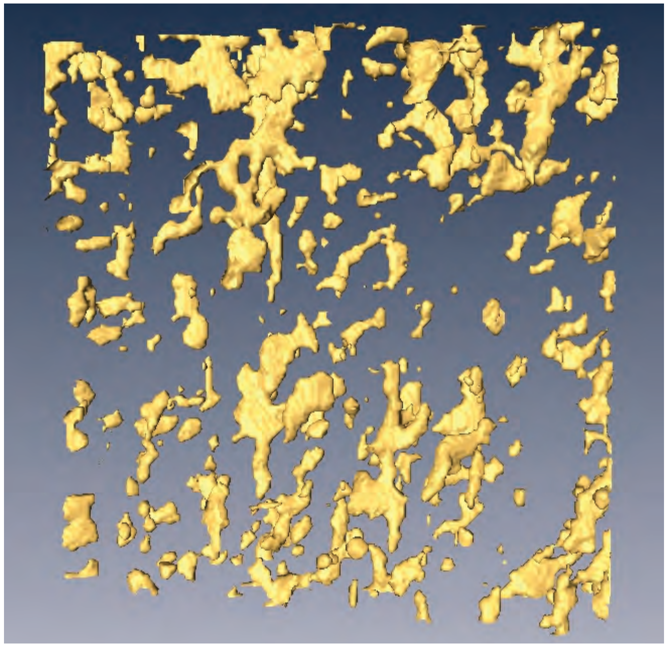

T = -15 °C, ϕ = 0.033

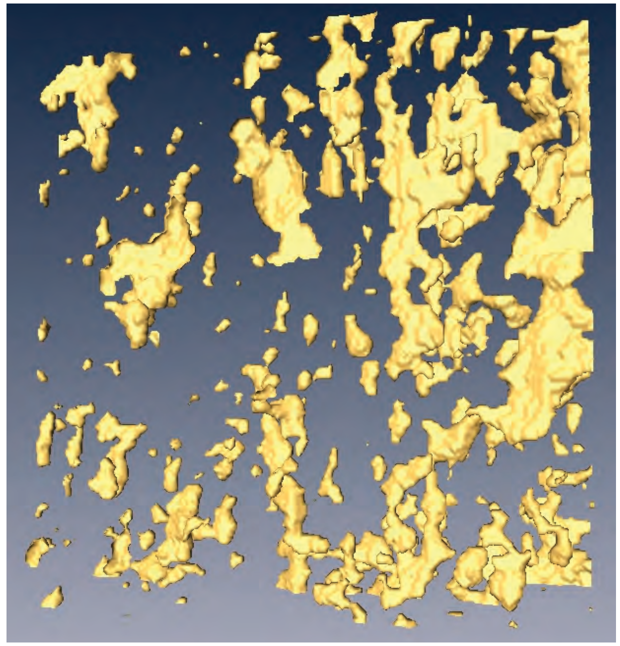

T = -6 °C, ϕ = 0.075

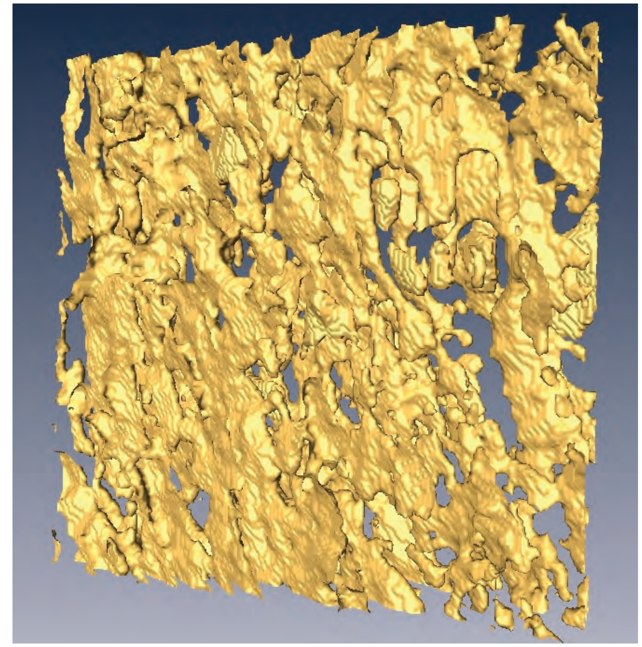

T = -3 °C, ϕ = 0.143

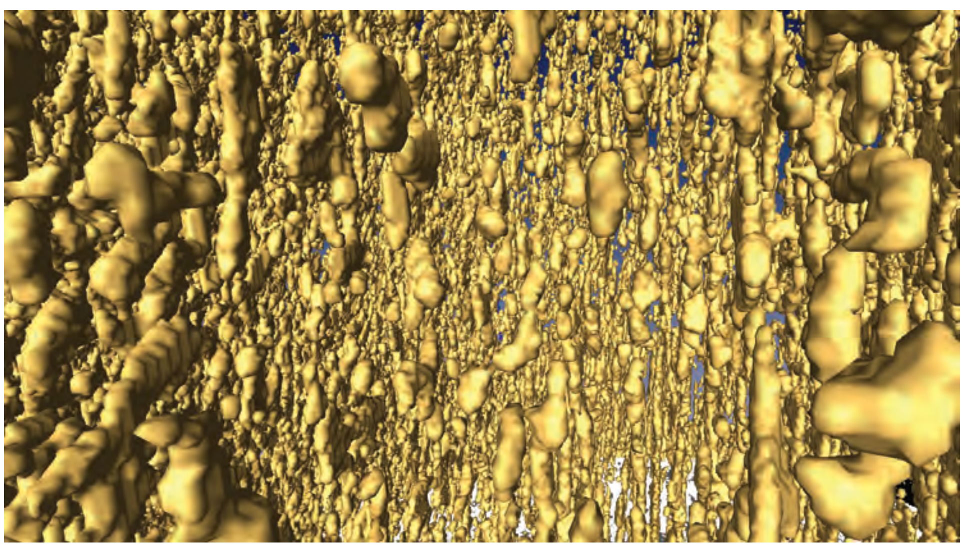

T = -8 °C, ϕ = 0.057

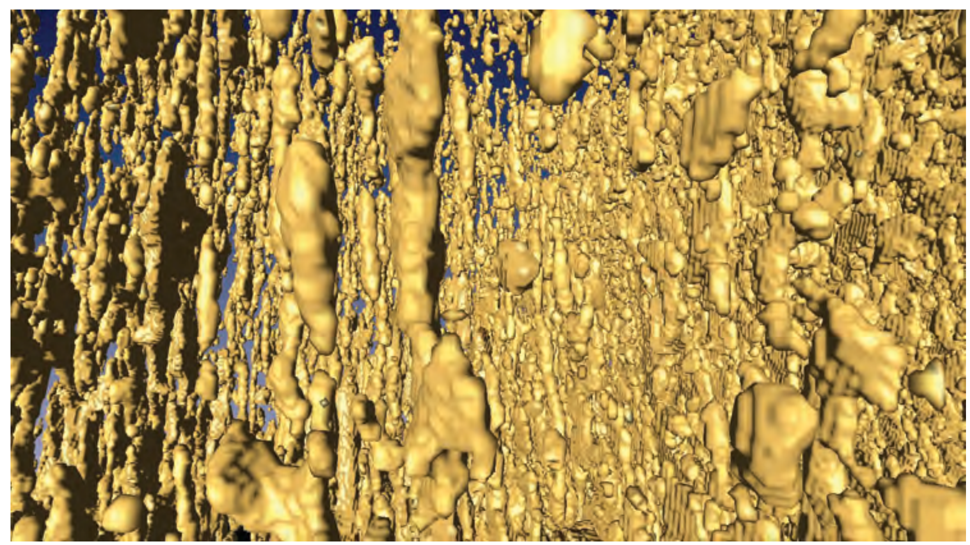

T = -4 °C, ϕ = 0.113

X-ray tomography for brine in sea ice

Golden *et al.*, *Geophysical Research Letters*, 2007

Critical behavior of fluid transport in sea ice

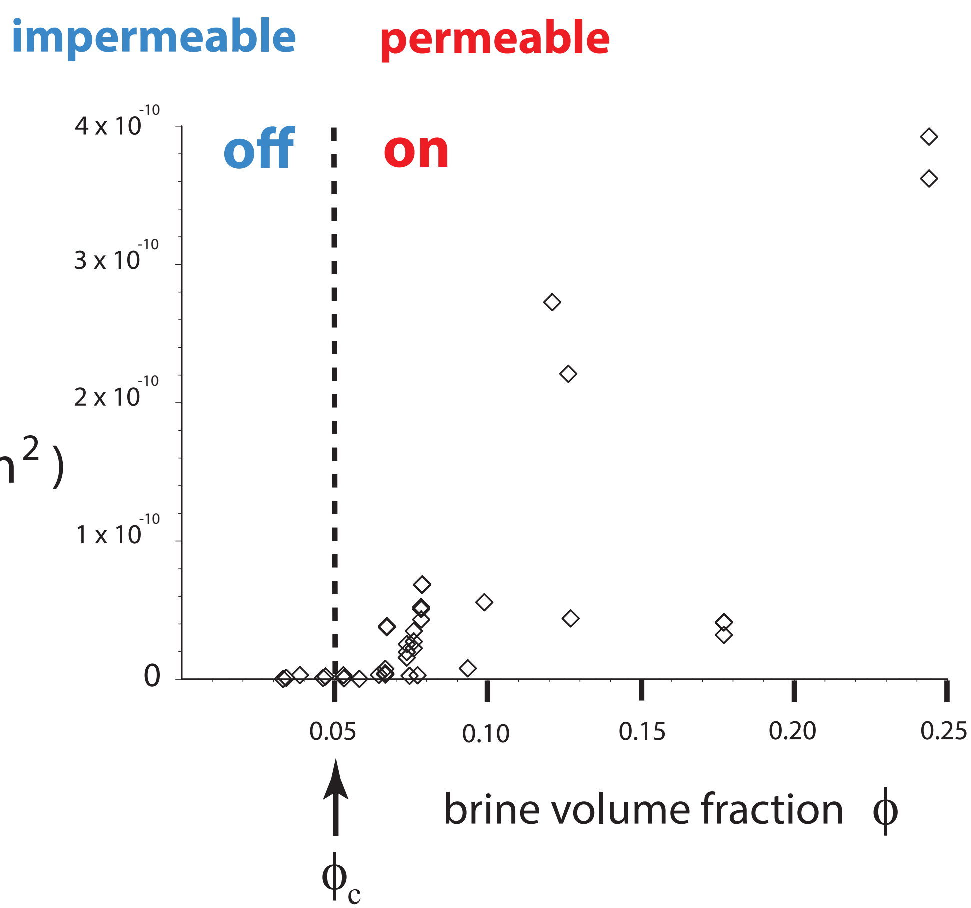

Arctic field data

vertical fluid permeability k (m^2)

"on - off" switch for fluid flow

critical brine volume fraction $\phi_c \approx 5\%$ $\longleftrightarrow$ $T_c \approx -5^\circ$C, $S \approx 5$ ppt

RULE OF FIVES

Golden, Ackley, Lytle Science 1998
Golden, Eicken, Heaton, Miner, Pringle, Zhu GRL 2007
Pringle, Miner, Eicken, Golden J. Geophys. Res. 2009

Thermal evolution of permeability and microstructure in sea ice

Golden, Eicken, Heaton*, Miner, Pringle, Zhu,   Geophysical Research Letters   2007

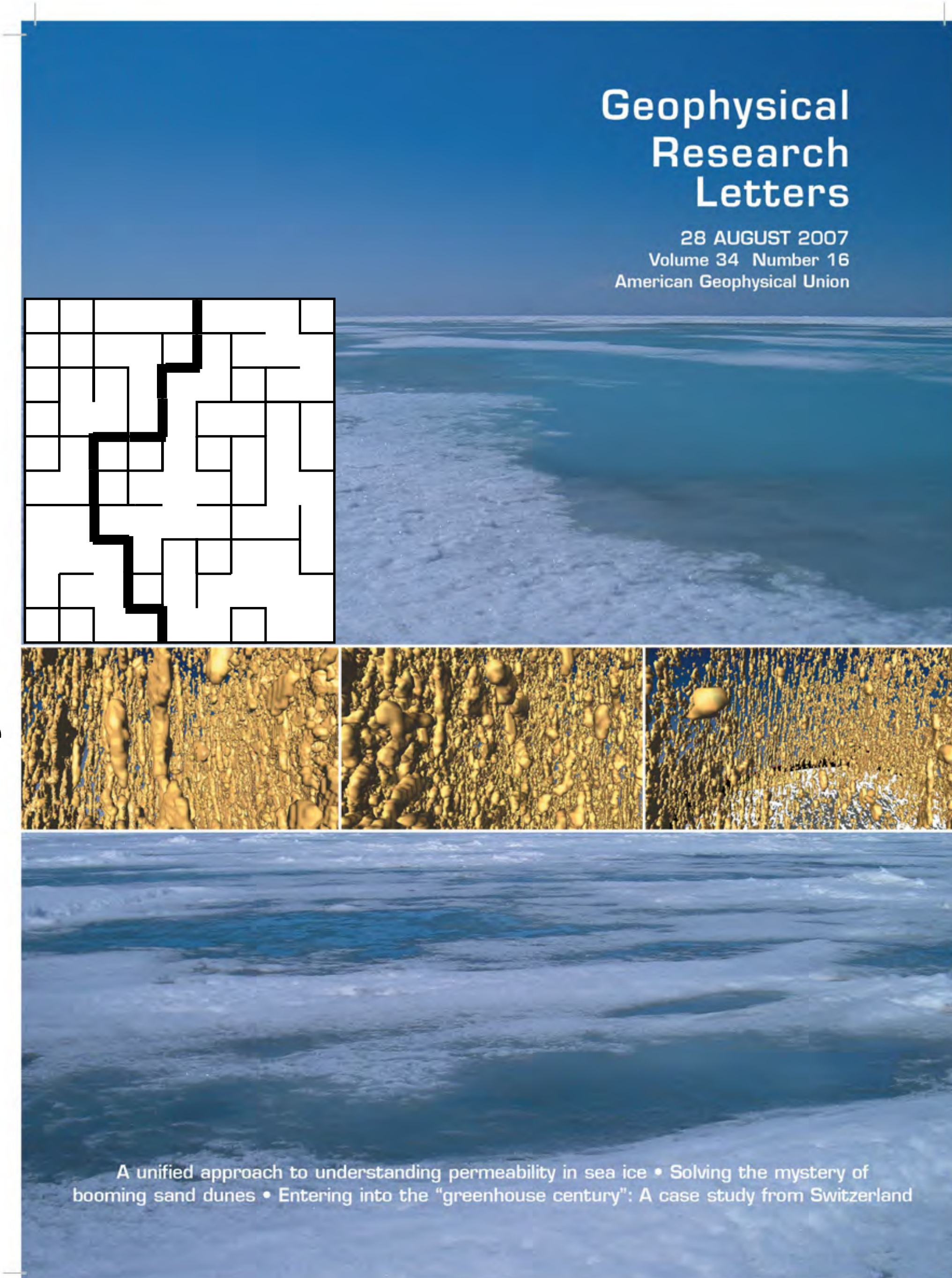

percolation theory for fluid permeability

$$k(\phi) = k_0 (\phi - 0.05)^2$$

critical exponent t

$$k_0 = 3 \times 10^{-8}\ \mathrm{m}^2$$

from critical path analysis in hopping conduction

hierarchical model
rock physics
network model
rigorous bounds

X-ray tomography for brine inclusions

confirms rule of fives

Pringle, Miner, Eicken, Golden J. Geophys. Res. 2009

theories agree closely with field data

microscale

governs

mesoscale processes

melt pond evolution

Sea ice algae secrete extracellular polymeric substances (EPS) affecting evolution of brine microstructure.

How does EPS affect fluid transport? **How does the biology affect the physics?**

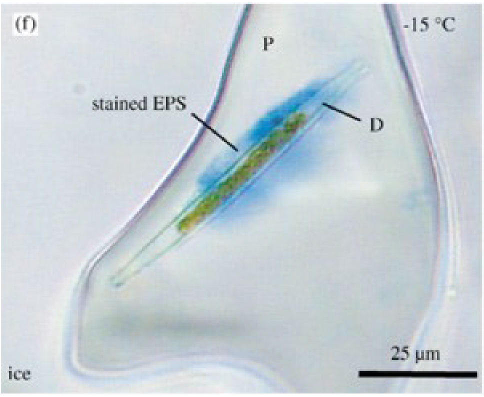

Krembs

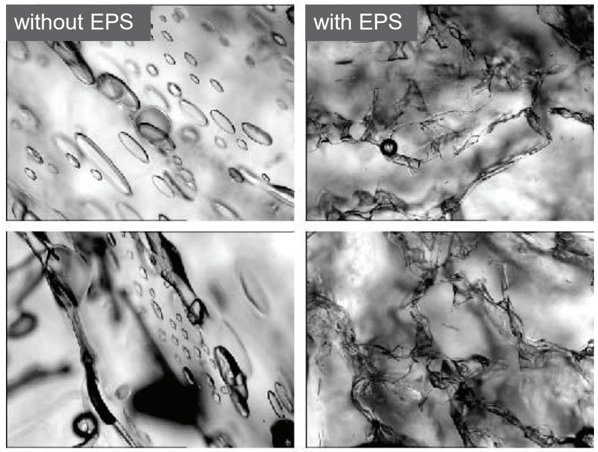

Krembs, Eicken, Deming, PNAS 2011

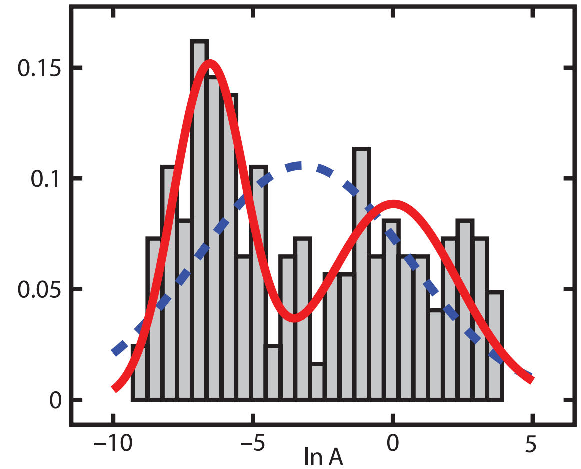

RANDOM PIPE MODEL

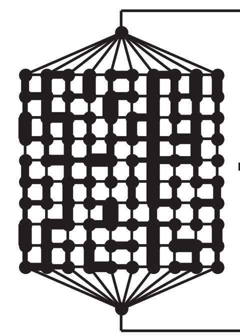

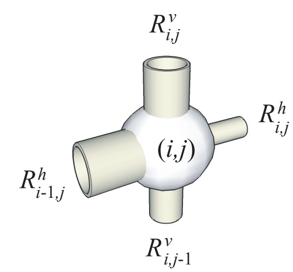

- 2D random pipe model with bimodal distribution of pipe radii

- Rigorous bound on permeability *k;* results predict observed drop in *k*

Steffen, Epshteyn, Zhu, Bowler, Deming, Golden
***Multiscale Modeling and Simulation*, 2018**

Zhu, Jabini, Golden, Eicken, Morris
Ann. Glac. 2006

Thermal evolution of the fractal geometry of the brine microstructure in sea ice

N. Ward, D. Hallman, H. Eicken, M. Oggier and K. M. Golden, 2022

$T = -12\ ^\circ C,\ \phi = 0.033$ $T = -8^\circ C,\ \phi = 0.057$

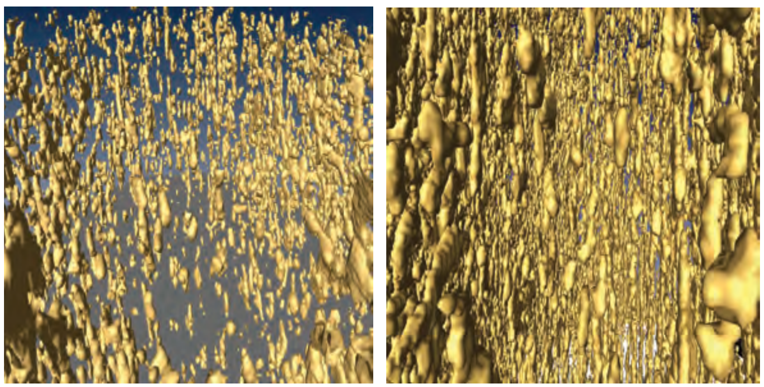

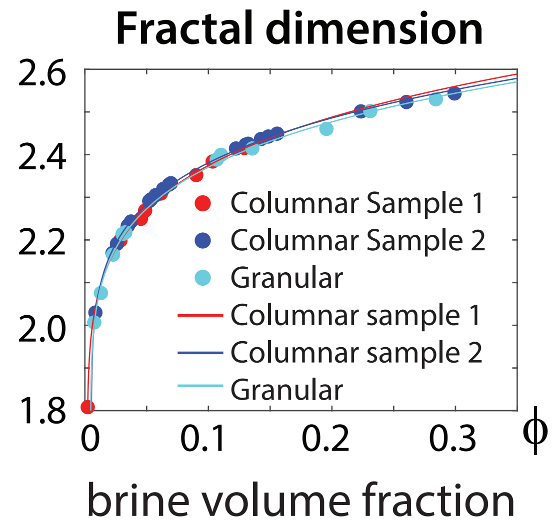

X-ray tomography DLA model

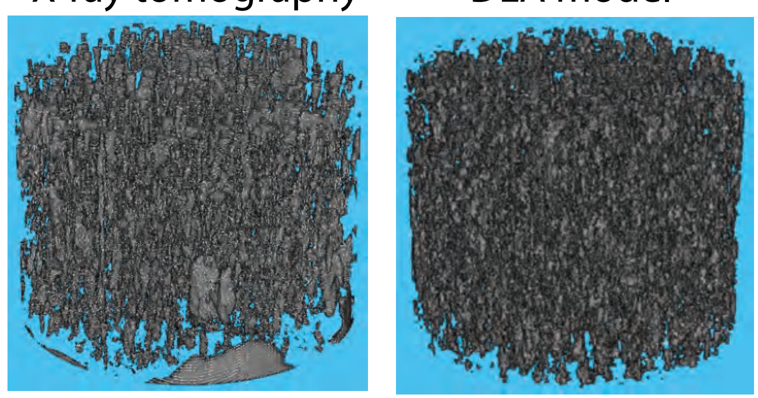

Remote sensing of sea ice

sea ice thickness
ice concentration

INVERSE PROBLEM

Recover sea ice properties from electromagnetic (EM) data

$$\varepsilon^*$$

effective complex permittivity
(dielectric constant, conductivity)

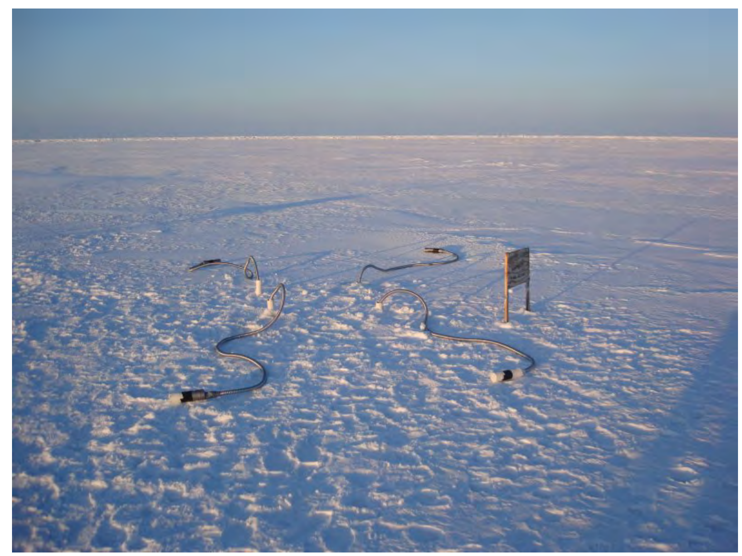

brine volume fraction
brine inclusion connectivity

Effective complex permittivity of a two phase composite in the quasistatic (long wavelength) limit

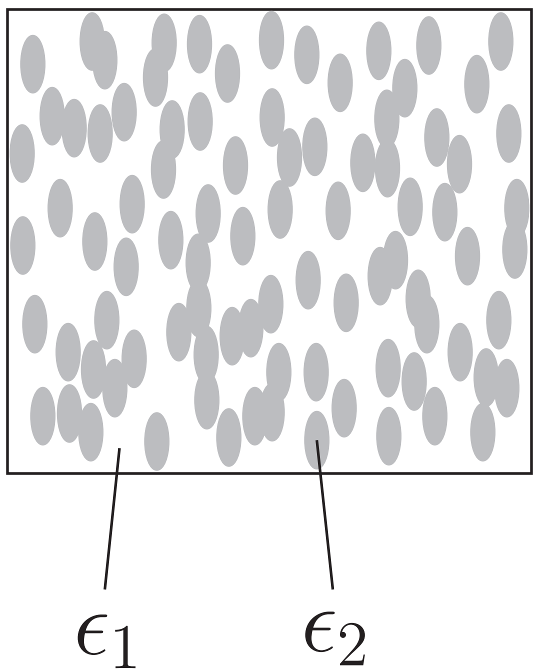

$$\Big\} \; \epsilon^*$$

$$D = \epsilon E$$

$$\nabla \cdot D = 0$$

$$\nabla \times E = 0$$

$$\langle D \rangle = \epsilon^* \langle E \rangle$$

p_1 , p_2 = volume fractions of the components

$$\epsilon^* = \epsilon^* \left(\frac{\epsilon_1}{\epsilon_2} \text{ , composite geometry } \right)$$

What are the effective propagation characteristics of an EM wave (radar, microwaves) in the medium?

Analytic Continuation Method for Homogenization

Bergman (1978), Milton (1979), Golden and Papanicolaou (1983), Theory of Composites, Milton (2002)

Stieltjes integral representation for homogenized parameter

separates geometry from parameters

geometry

$$F(s) = 1 - \frac{\epsilon^*}{\epsilon_2} = \int_0^1 \frac{d\mu(z)}{s - z}$$

$$s = \frac{1}{1 - \epsilon_1 / \epsilon_2}$$

material parameters

μ
- spectral measure of self adjoint operator $\Gamma\chi$
- mass $= p_1$
- higher moments depend on n-point correlations

$$\Gamma = \nabla(-\Delta)^{-1}\nabla\cdot$$

$\chi =$ characteristic function of the brine phase

$$E = s\,(s + \Gamma\chi)^{-1} e_k$$

$\Gamma\chi$: microscale $\longrightarrow$ macroscale

$\Gamma\chi$ *links scales*

Forward and inverse bounds on the complex permittivity of sea ice

Golden and Papanicolaou, Comm. Math. Phys. 1983

Bounds on the complex permittivity of polycrystalline materials by analytic continuation

Adam Gully, Joyce Lin,
Elena Cherkaev, Ken Golden

- **Stieltjes integral representation for effective complex permittivity**

  Milton (1981, 2002), Barabash and Stroud (1999), ...
- **Forward and inverse bounds**

  orientation statistics
- **Applied to sea ice using two-scale homogenization**
- **Inverse bounds give method for distinguishing ice types using remote sensing techniques**


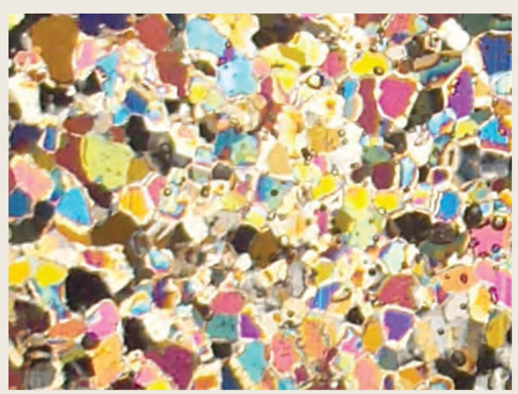

Proc. Roy. Soc. A 8 Feb 2015

wave propagation in the marginal ice zone (MIZ)

first theory of key parameter in wave-ice interactions only fitted to wave data before

Keller, 1998
Mosig, Montiel, Squire, 2015
Wang, Shen, 2012

Analytic Continuation Method

Bergman (78) - Milton (79)
integral representation for ε^*
Golden and Papanicolaou (83)

Milton, *Theory of Composites* (02)

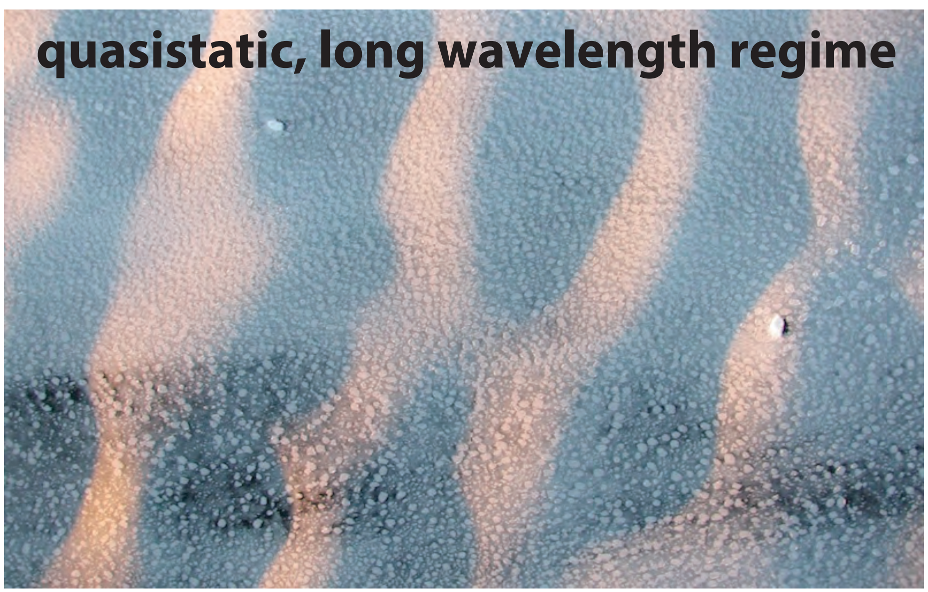

homogenized parameter depends on sea ice concentration and ice floe geometry

like EM waves

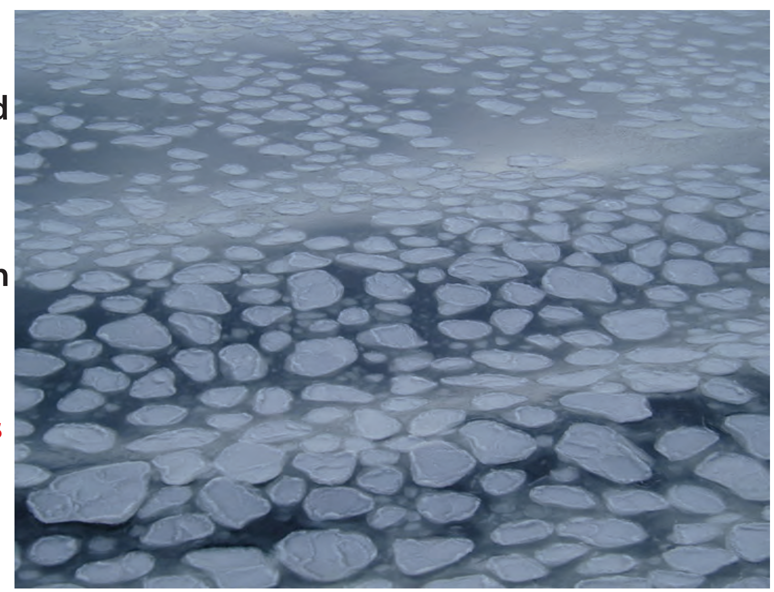

Spectral computations for sea ice floe configurations

spectral measures

eigenvalue spacing distributions

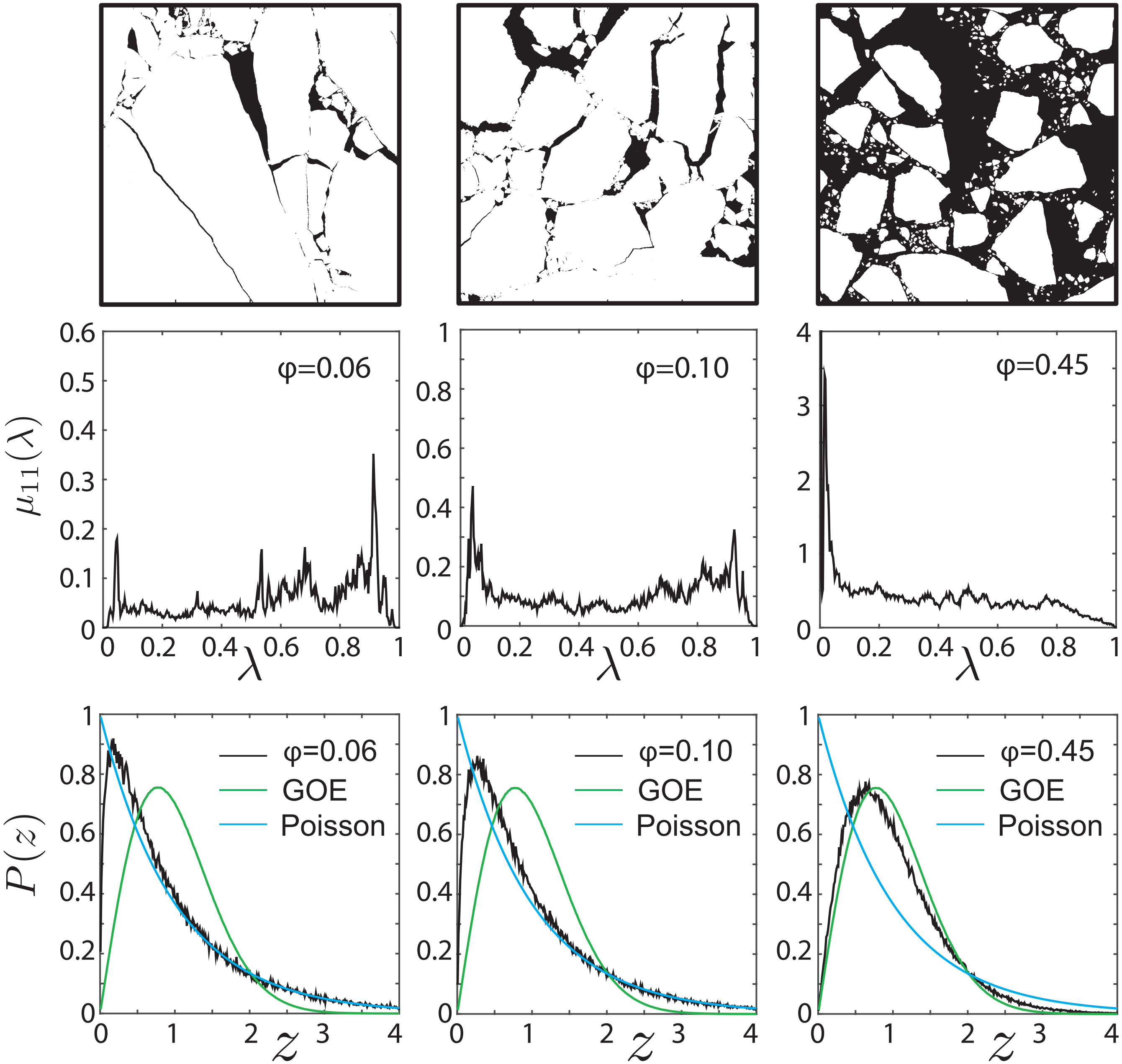

uncorrelated → **level repulsion**

UNIVERSAL Wigner-Dyson distribution

Anderson localization transition

Murphy, Cherkaev, Golden, Phys. Rev. Lett. 2017

Order to Disorder in Quasiperiodic Composites

David Morison (Physics & Astronomy), Ben Murphy, Elena Cherkaev, Ken Golden, Comm. Physics, 2022

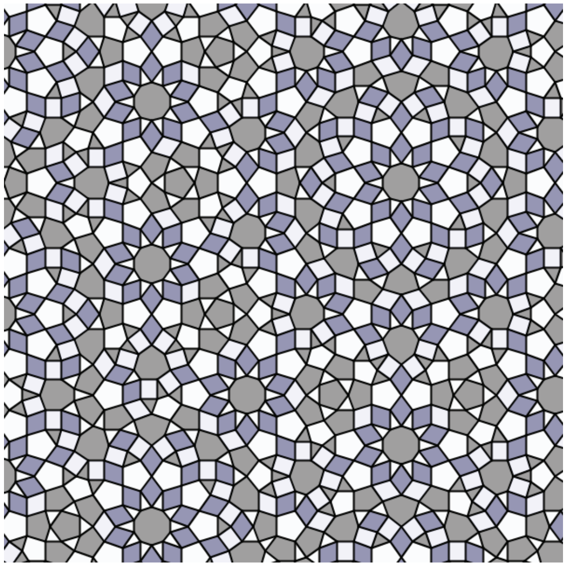

quasiperiodic checkerboard

Stampfli, 2013

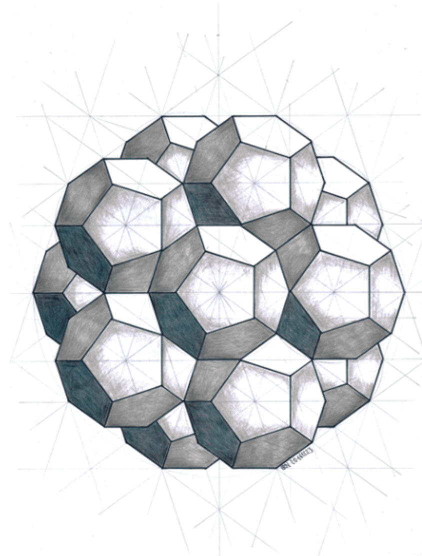

dense packing of dodecahedra

3D Penrose tiling

Tripkovic, 2019

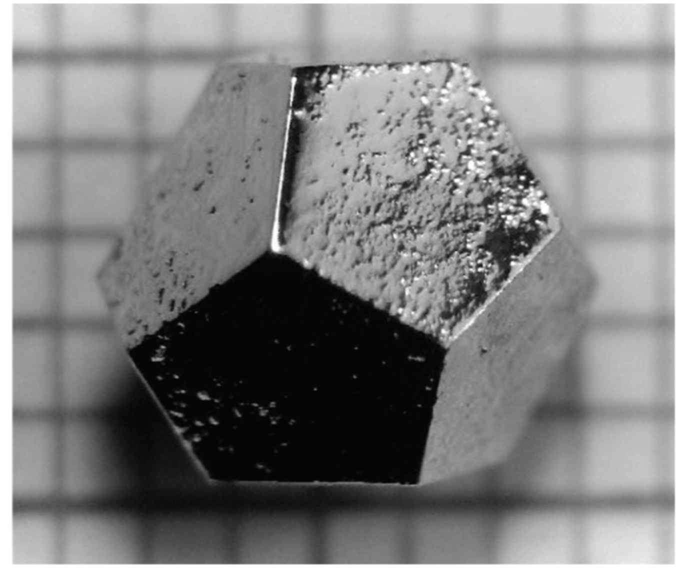

Holmium–magnesium–zinc quasicrystal

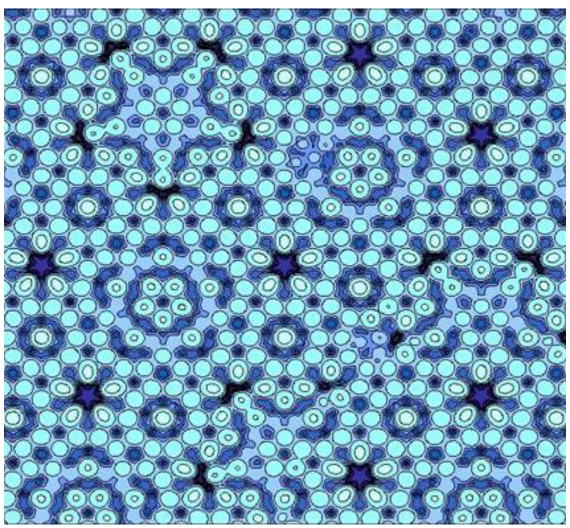

energy surface Al-Pd-Mn quasicrystal

Unal et al., 2007

quasiperiodic crystal

quasicrystal

ordered but aperiodic

lacks translational symmetry

Schechtman et al., 1984

Levine & Steinhardt, 1984

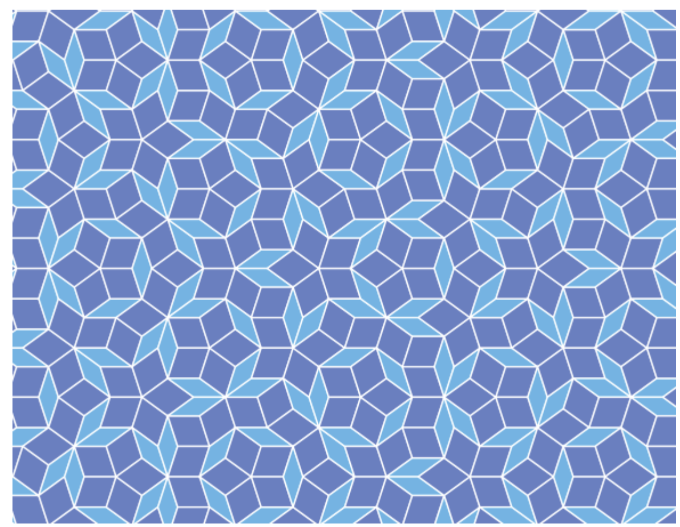

aperiodic tiling of the plane - R. Penrose 1970s

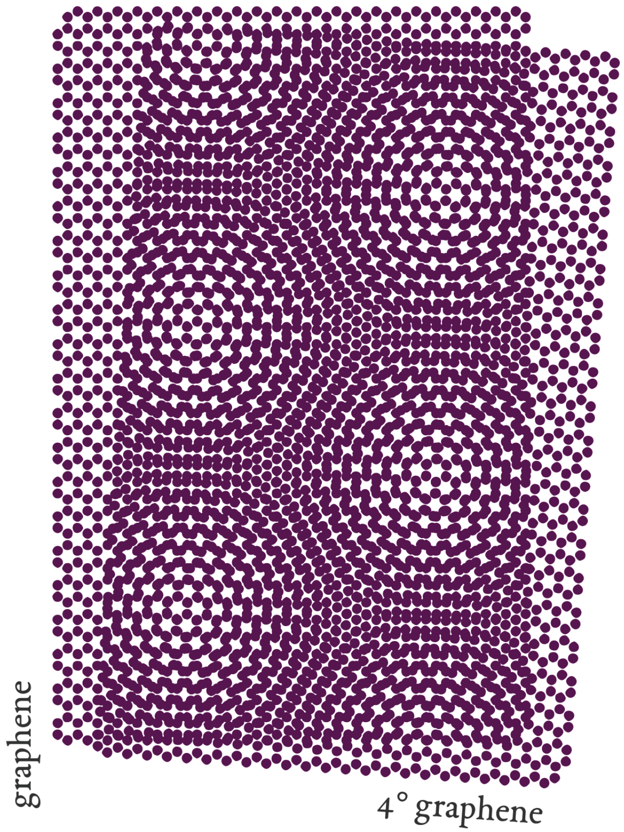

twisted bilayer graphene

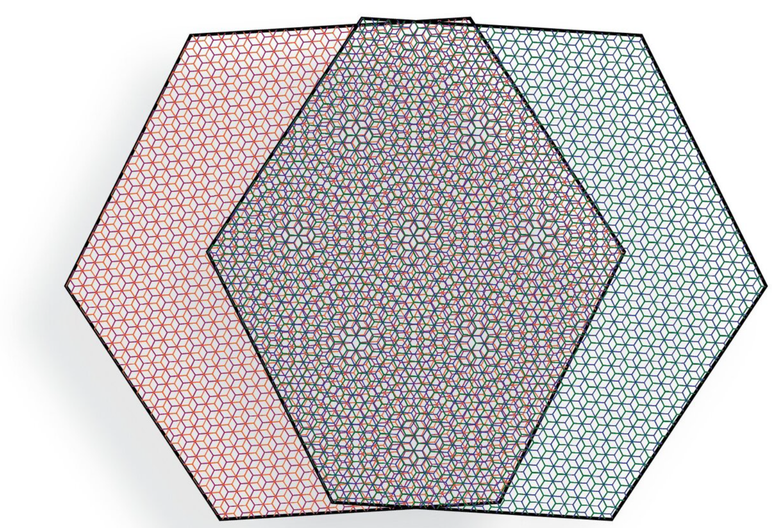

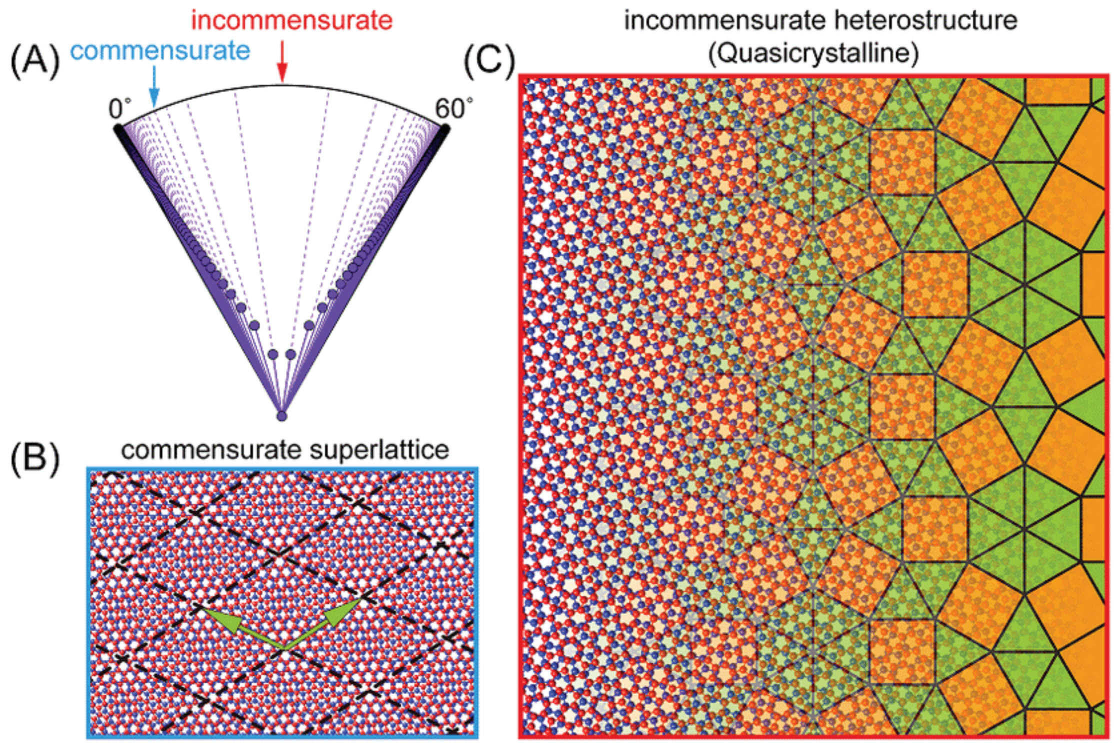

Yao et al., 2018

Order to disorder in quasiperiodic composites

Morison, Murphy, Cherkaev, Golden, Comm. Phys. 2022

Parameterized Moiré Pattern Creates Tunable Microgeometry

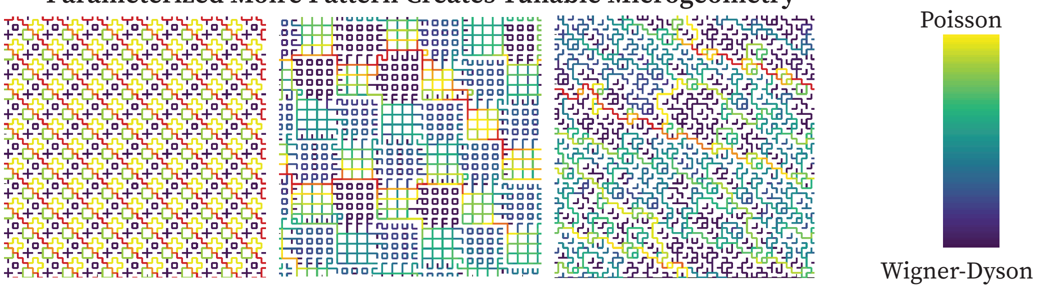

constellation of periodic systems in a sea of randomness

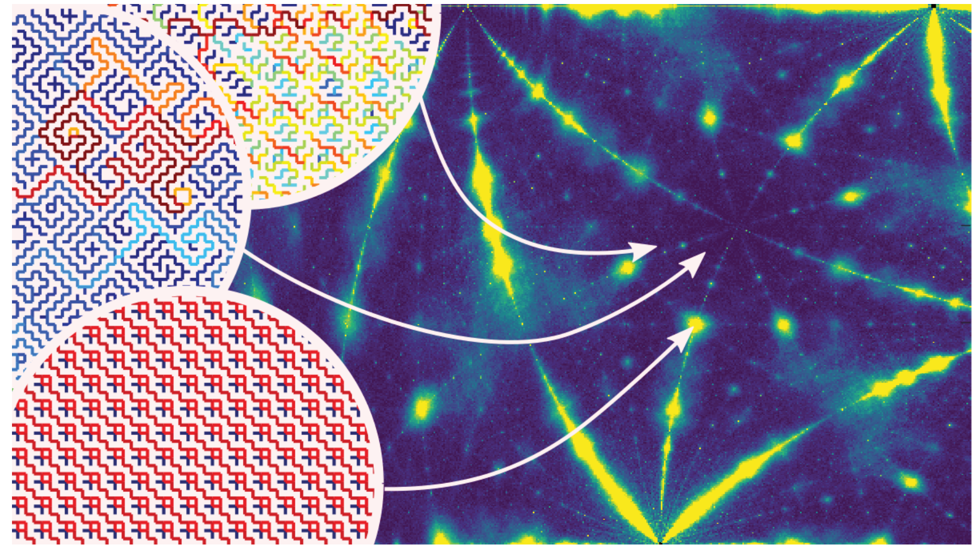

Moiré parameter space

periodic → quasiperiodic

electric field strength

spectral measure

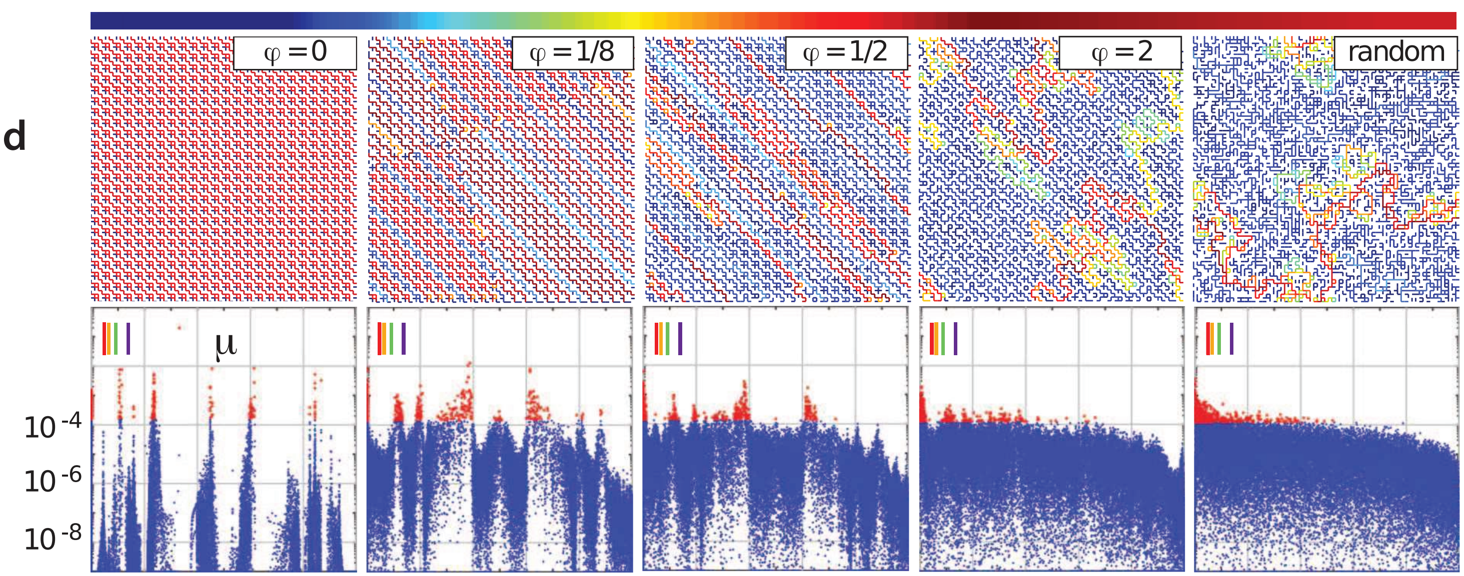

RRN at percolation threshold

we bring the framework of solid state physics of electronic transport and band gaps in semiconductors to classical transport in periodic and quasiperiodic composites

Anderson transition as twist angle is tuned

photonic crystals and quasicrystals

Fractal arrangement of periodic systems

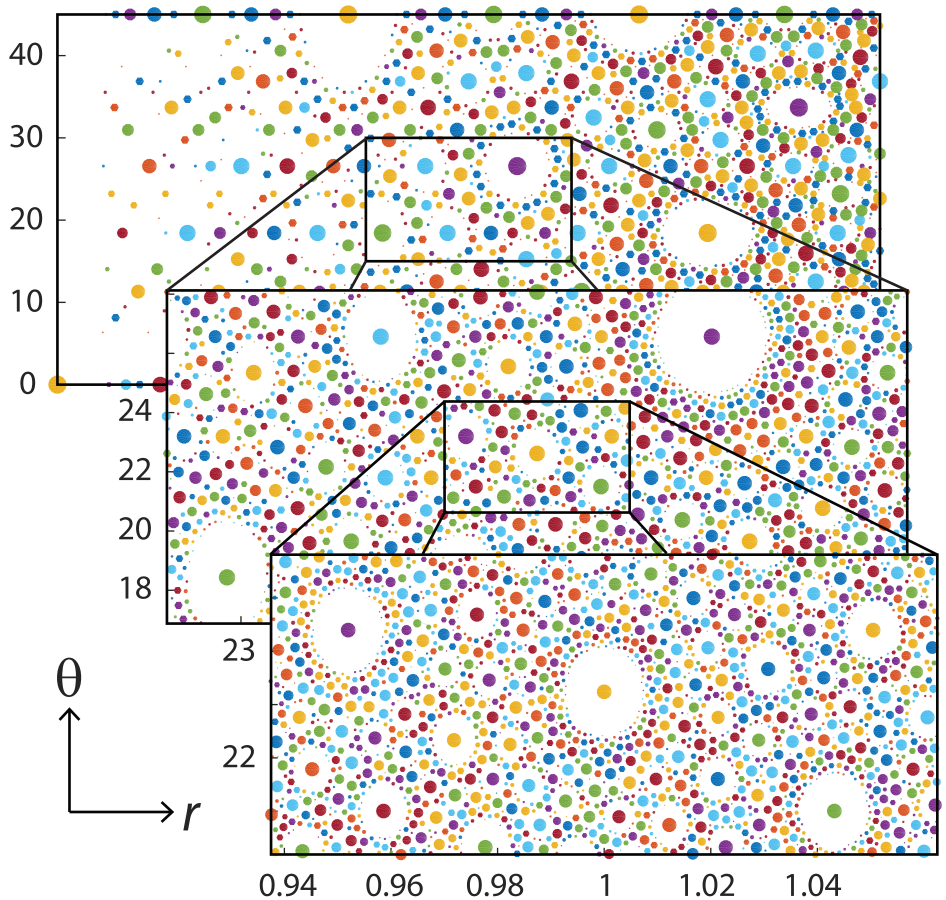

Sequential insets zooming into smaller regions of parameter space.

size of the dots ~ length of period

(large dot ~ small period; small dot ~ large period; white space ~ "infinite" period)

mesoscale

melt pond formation and albedo evolution:

- ***major drivers in polar climate***
- ***key challenge for global climate models***

numerical models of melt pond evolution, including topography, drainage (permeability), etc.

Lüthje, Feltham, Taylor, Worster 2006

Flocco, Feltham 2007

Skyllingstad, Paulson, Perovich 2009

Flocco, Feltham, Hunke 2012

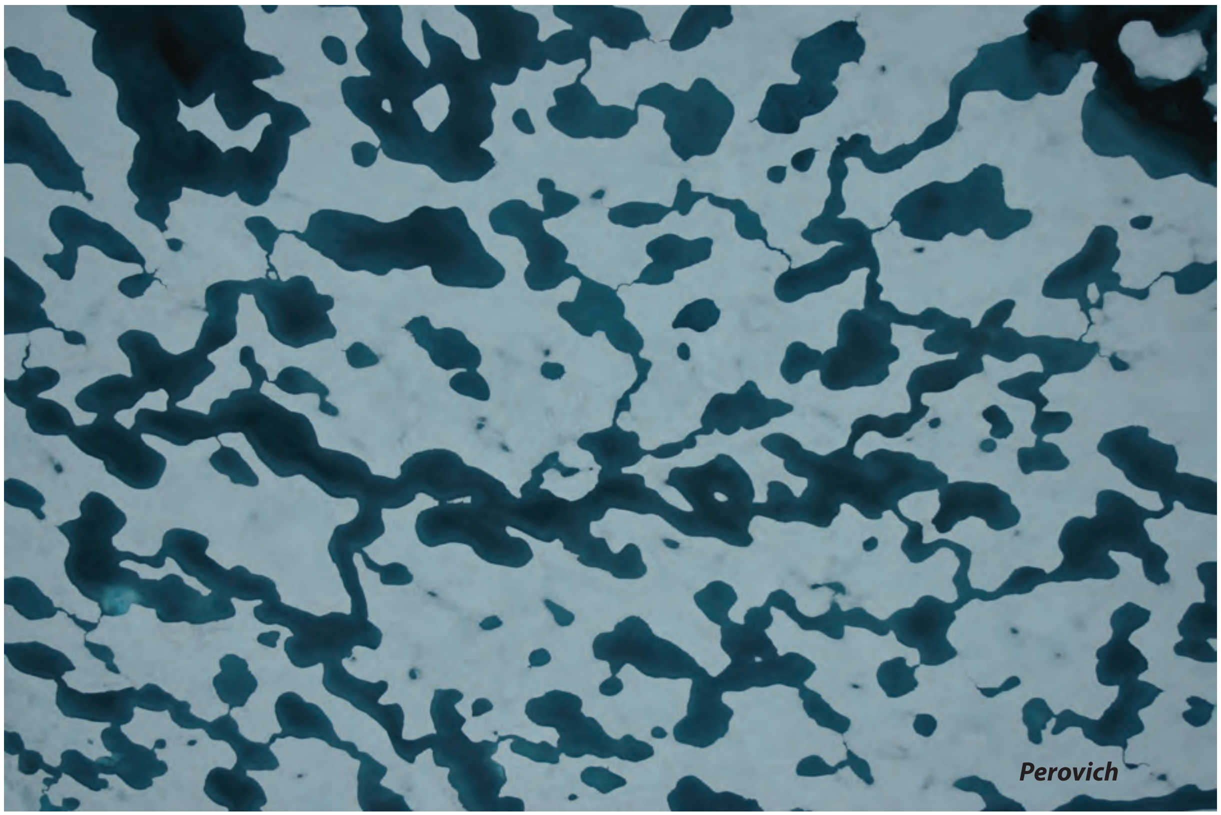

Are there universal features of the evolution similar to phase transitions in statistical physics?

fractal curves in the plane

they wiggle so much that their dimension is >1

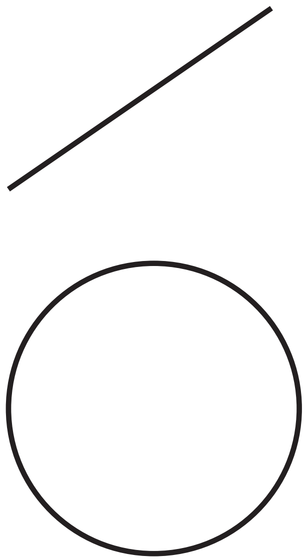

simple curves

D = 1

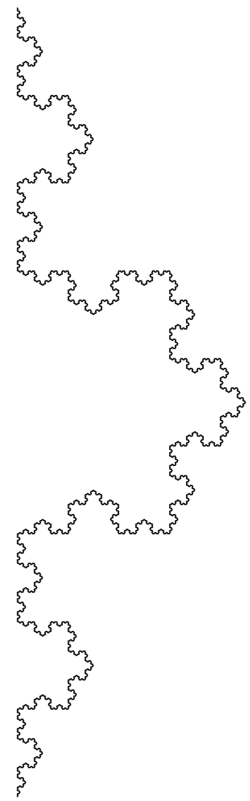

Koch snowflake

D = 1.26

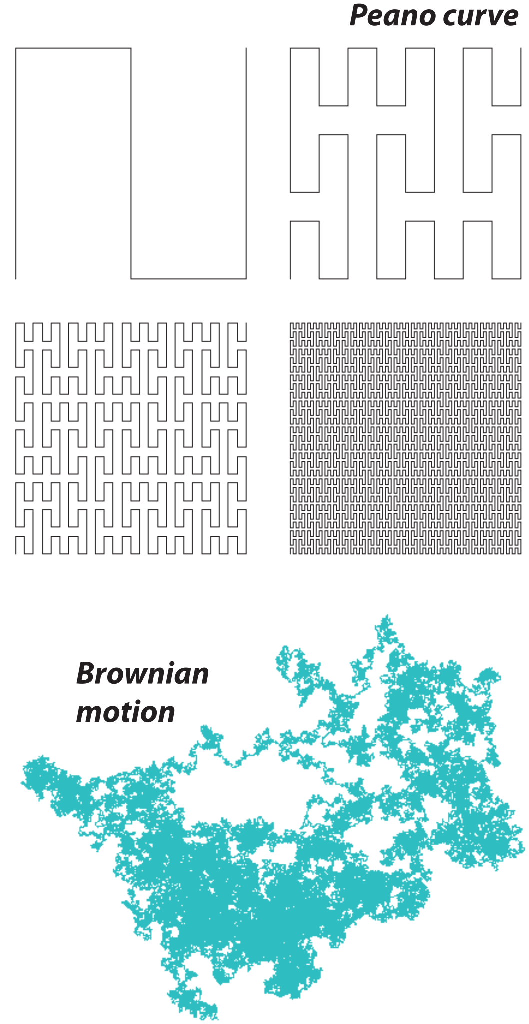

space filling curves

D = 2

Transition in the fractal geometry of Arctic melt ponds

Christel Hohenegger, Bacim Alali, Kyle Steffen, Don Perovich, Ken Golden

The Cryosphere, 2012

complexity grows with length scale

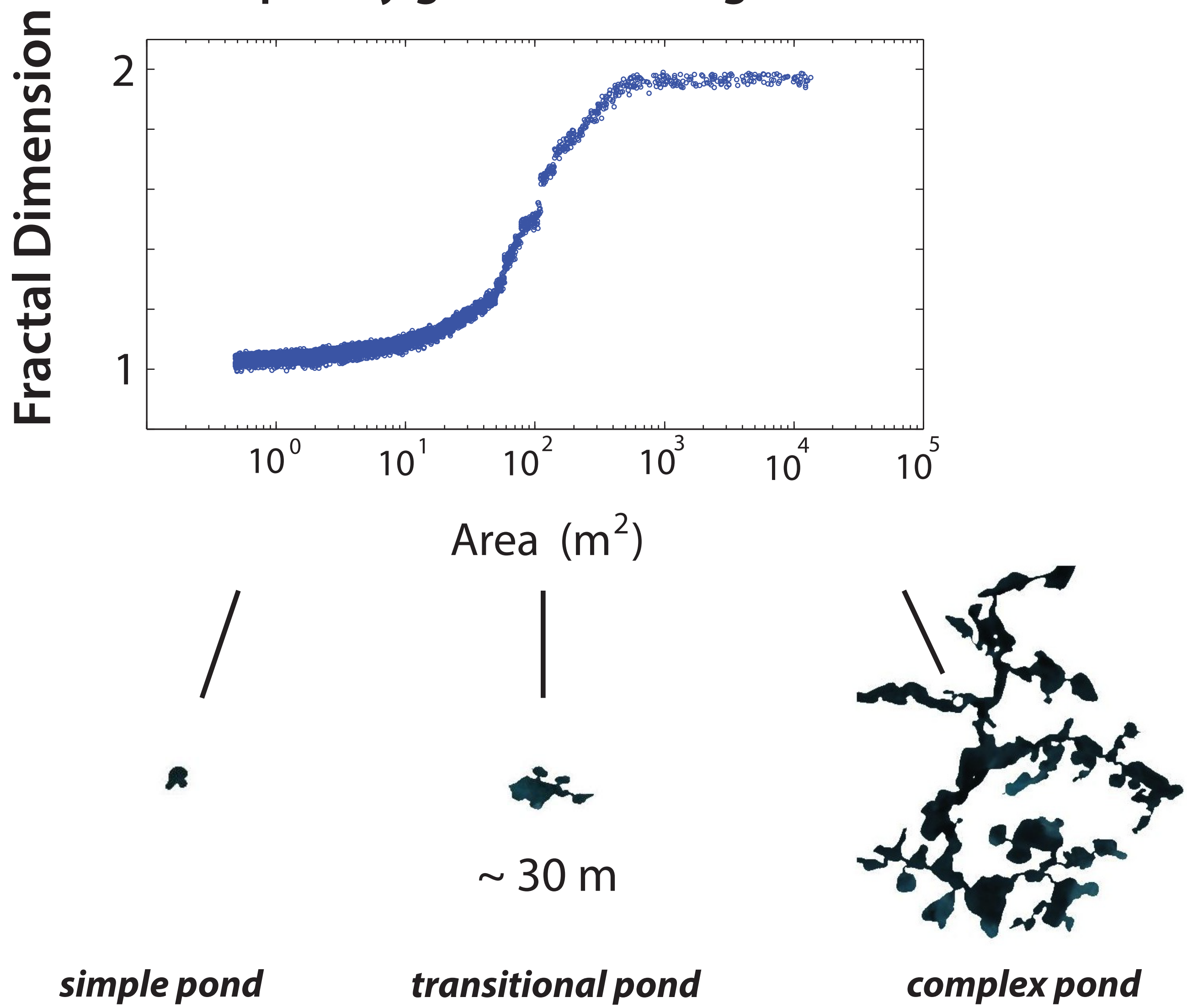

Continuum percolation model for melt pond evolution

level sets of random surfaces

Brady Bowen, Court Strong, Ken Golden, J. Fractal Geometry 2018

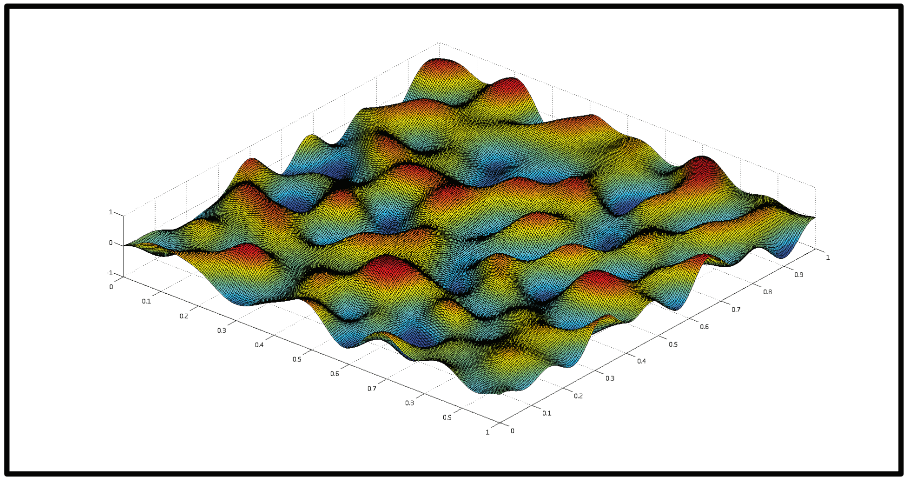

random Fourier series representation of surface topography

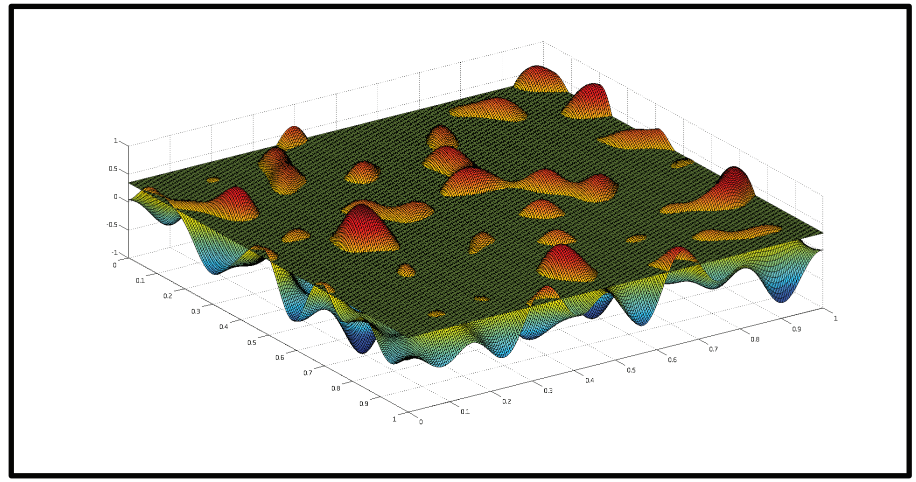

intersections of a plane with the surface define melt ponds

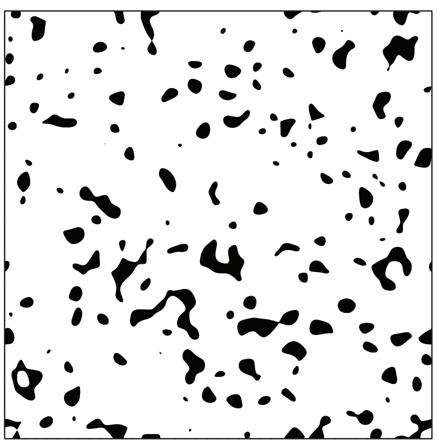

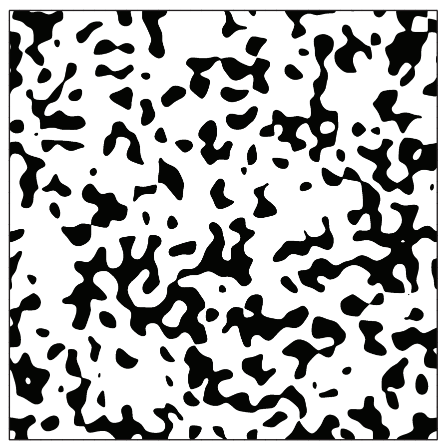

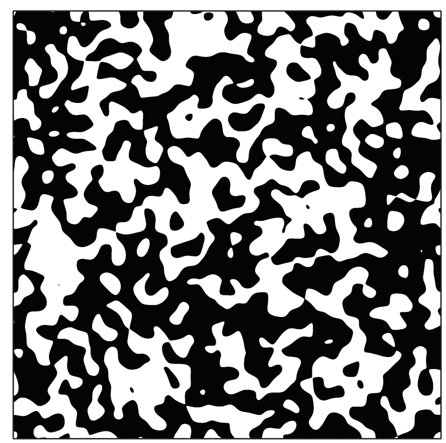

electronic transport in disordered media

diffusion in turbulent plasmas

Isichenko, Rev. Mod. Phys., 1992

Ising model for ferromagnets ⟶ Ising model for melt ponds

Ma, Sudakov, Strong, Golden, *New J. Phys.*, 2019

$$\mathcal{H} = -\sum_{i}^{N} H_i\, s_i - J \sum_{<i,j>}^{N} s_i s_j \qquad s_i = \begin{cases} \uparrow & +1 \quad \text{water} \quad \text{(spin up)} \\ \downarrow & -1 \quad \text{ice} \quad \text{(spin down)} \end{cases}$$

random magnetic field represents snow topography

magnetization M

pond area fraction *~ albedo*

$$F = \frac{(M+1)}{2}$$

only nearest neighbor patches interact

Starting with random initial configurations, as Hamiltonian energy is minimized by Glauber spin flip dynamics, system "flows" toward metastable equilibria.

Order from Disorder

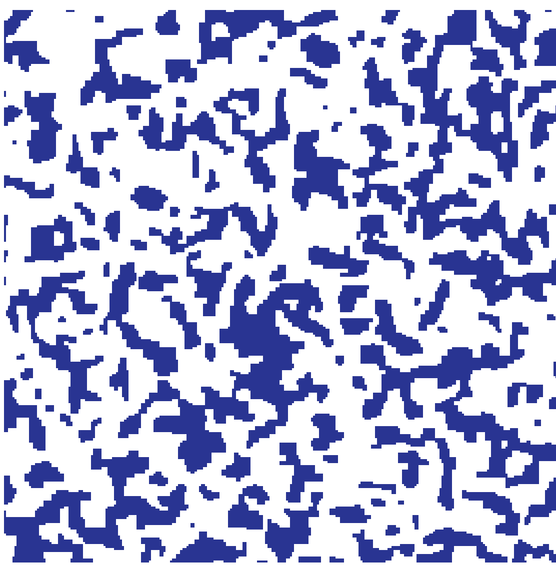

Ising model

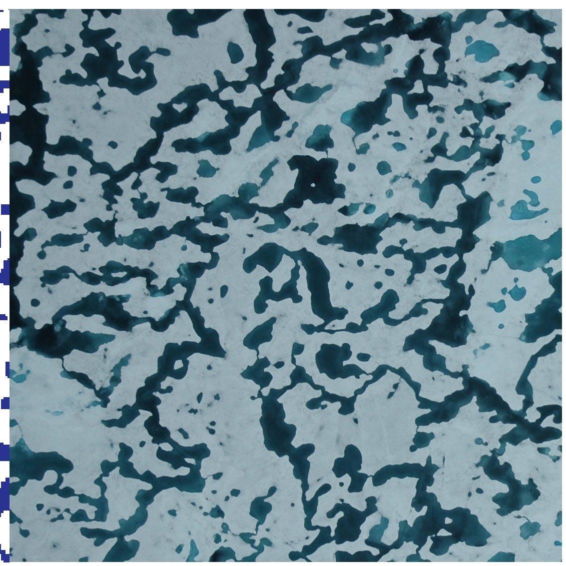

melt pond photo (Perovich)

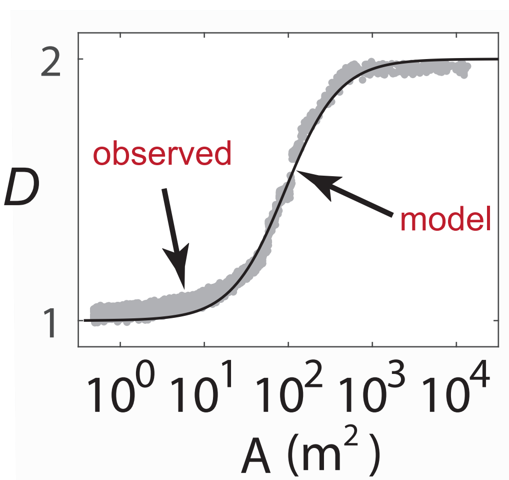

pond size distribution exponent

observed -1.5

(Perovich, *et al.* 2002)

model -1.58

Scientific American
EOS, PhysicsWorld, ...

ONLY MEASURED INPUT = LENGTH SCALE (GRID SIZE) from snow topography data

Perovich

Melt ponds control transmittance of solar energy through sea ice, impacting upper ocean ecology.

WINDOWS

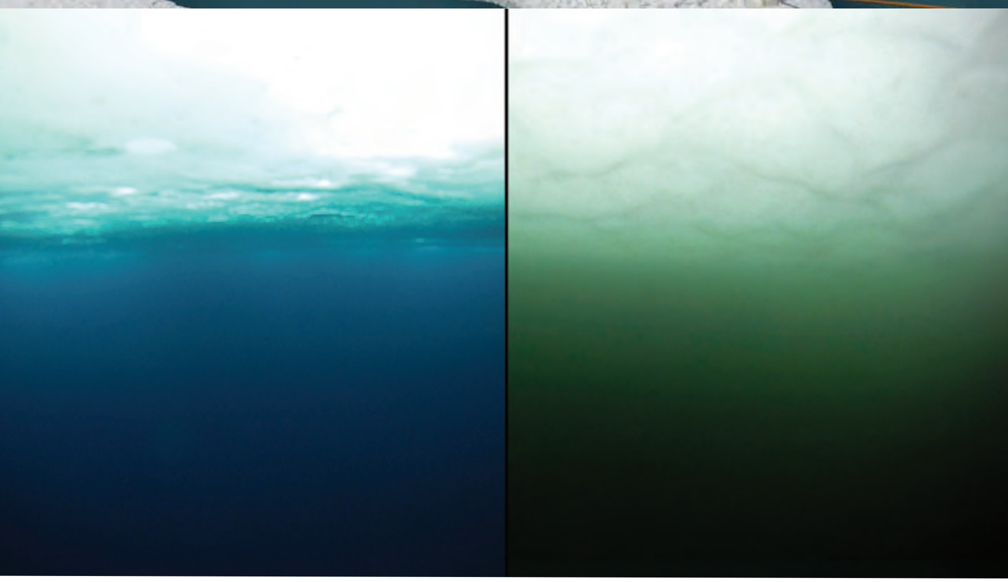

no bloom | bloom

massive under-ice algal bloom

Arrigo et al., *Science* 2012

Have we crossed into a new ecological regime?

The frequency and extent of sub-ice phytoplankton blooms in the Arctic Ocean

Horvat, Rees Jones, Iams, Schroeder, Flocco, Feltham, ***Science Advances*** 2017

The effect of melt pond geometry on the distribution of solar energy under first year sea ice

Horvat, Flocco, Rees Jones, Roach, Golden
Geophys. Res. Lett. 2019

(2015 AMS MRC)

SEA ICE ALGAE

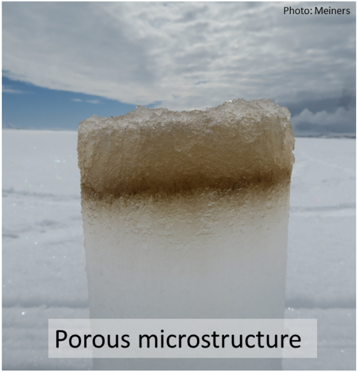

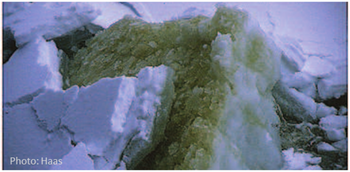

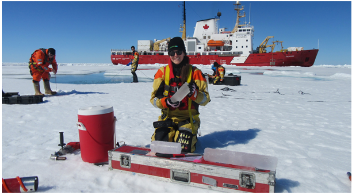

80% of polar bear diet can be traced to ice algae*.

* Brown TA, et al. (2018). *PloS one*, 13(1), e0191631

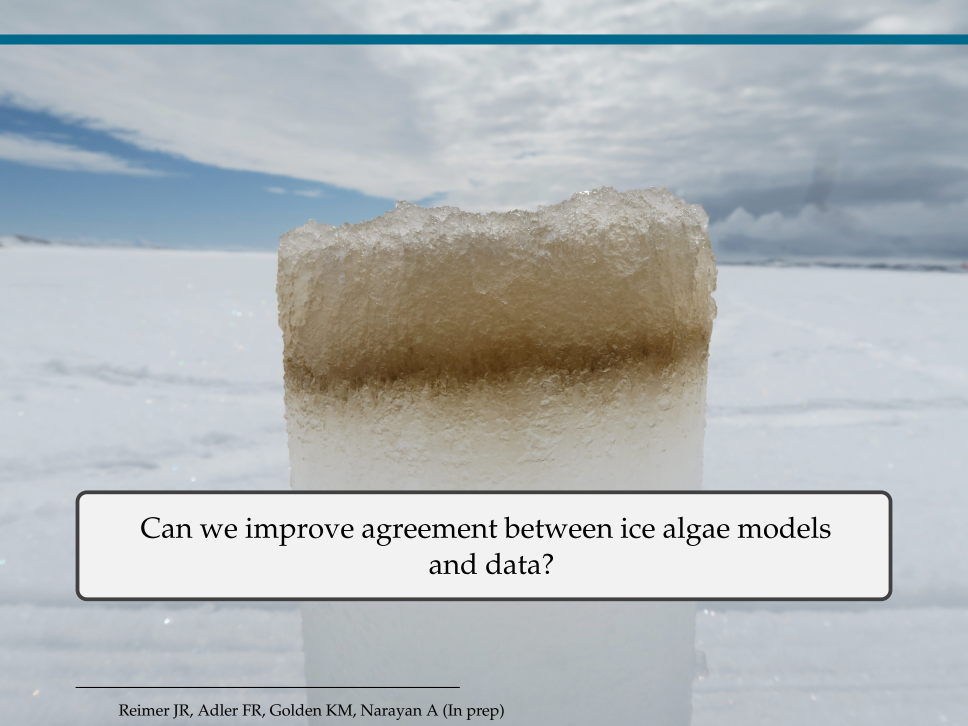

Can we improve agreement between ice algae models and data?

Reimer JR, Adler FR, Golden KM, Narayan A (In prep)

HETEROGENEITY

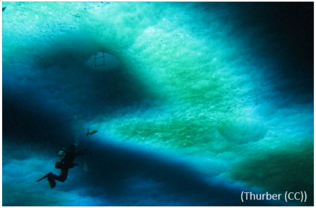

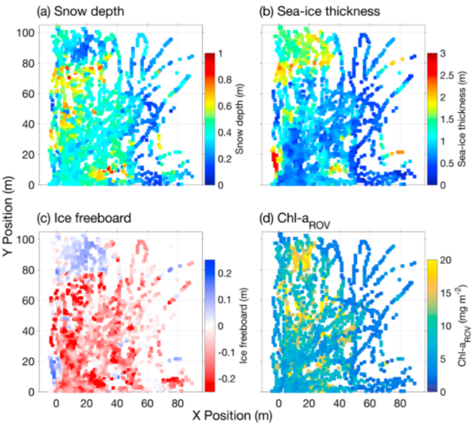

Meiners, K.M., et al. (2017). *Geophysical Research Letters*, 44(14), 7382-7390

Heterogeneity in initial conditions

At each location within a larger region, we could consider

$$\text{nutrients} \qquad \frac{dN}{dt} = \alpha - BNP - \eta N$$

$$\text{algae} \qquad \frac{dP}{dt} = \gamma BNP - \delta P$$

$$N(0) = N_0, \qquad P(0) = P_0$$

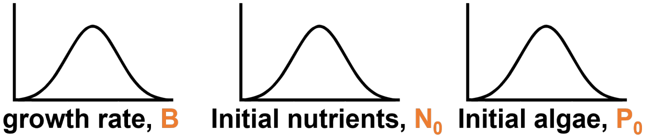

How do we analyze this model?

Monte Carlo simulations?

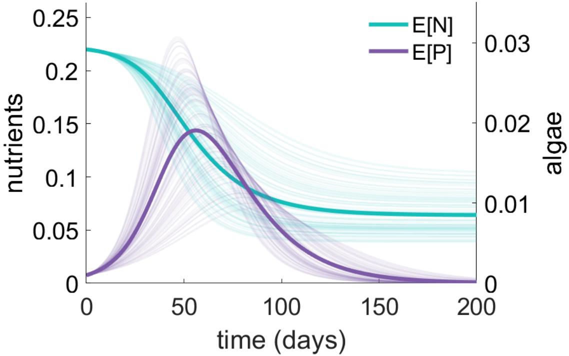

Too slow! Full algae model takes **8 hours** (cloud computing).

Uncertainty quantification and ecological dynamics in a model of a sea ice algae bloom, in prep. 2022

Jody Reimer, Fred Adler, Ken Golden, and Akil Narayan

POLYNOMIAL CHAOS EXPANSIONS (D. Xiu, 2010)
nonintrusive methods for building PC expansions

Ecological insights

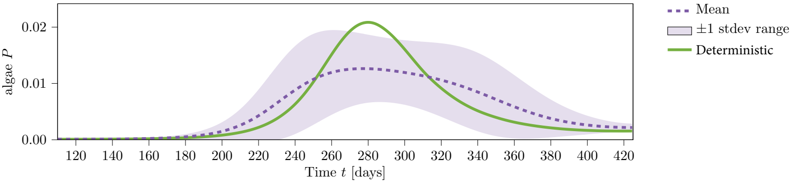

- lower peak bloom intensity
- longer bloom duration
- able to compare variance to data

macroscale

Anomalous diffusion in sea ice dynamics

Ice floe diffusion in winds and currents

observations from GPS data:

Jennifer Lukovich, Jennifer Hutchings, David Barber, *Ann. Glac.* 2015

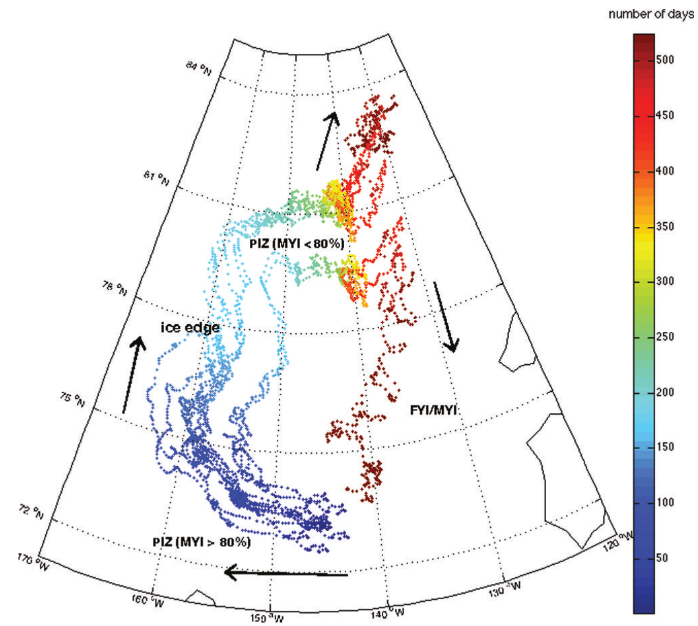

- **On short time scales floes observed (buoy data) to exhibit Brownian-like behavior, but they are also being advected by winds and currents.**
- **Effective behavior is purely diffusive, sub-diffusive or super-diffusive depending on ice pack and advective conditions - Hurst exponent.**

modeling:

Huy Dinh, Ben Murphy, Elena Cherkaev, Court Strong, Ken Golden 2022

floe scale model to analyze transport regimes in terms of ice pack crowding, advective conditions

Delaney Mosier, Jennifer Hutchings, Jennifer Lukovich, Marta D'Elia, George Karniadakis, Ken Golden 2022

learning fractional PDE governing diffusion from data

Model larger scale effective behavior with partial differential equations that *homogenize* complex local structure and dynamics.

Arctic MIZ

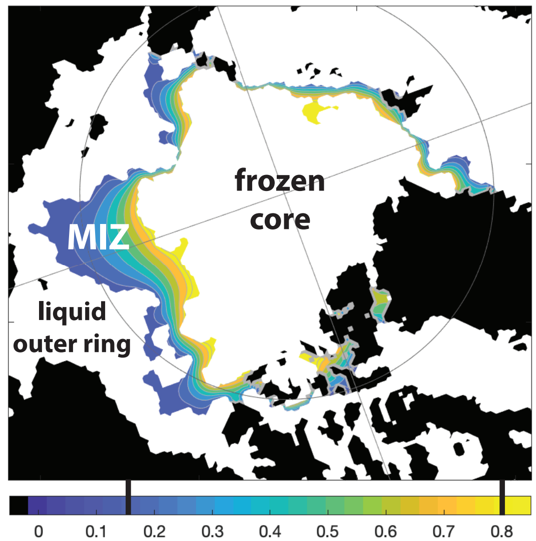

sea ice concentration ψ

Predict MIZ width and location with basin-scale phase change model.

dynamic transitional region - mushy layer - separating two “pure” phases

seasonal and long term trends

C. Strong, E. Cherkaev, and K. M. Golden,
Annual cycle of Arctic marginal ice zone location
and width explained by phase change front model, 2022

Learning the velocity field in an advection diffusion model for sea ice concentration

Delaney Mosier, Court Strong, Elena Cherkaev, Ken Golden, 2022
Eric Brown, Delaney Mosier, Bao Wang, Ken Golden, 2022

Goal: Develop PDE model to describe evolution of sea ice concentration field.

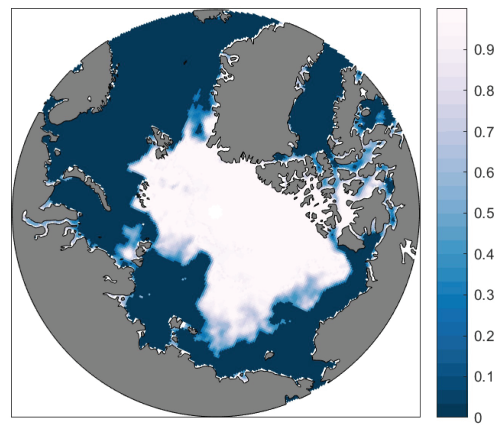

National Snow and Ice Data Center

discretized satellite concentration data

Figure 1. Arctic sea ice concentration in early August 2012.

advection diffusion model for sea ice concentration:

$$\frac{\partial \psi}{\partial t} = -\mathbf{v} \cdot \nabla \psi + k \Delta \psi$$

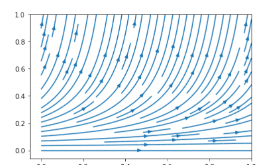

learned velocity

2.5% absolute error in preliminary study

Use two-layer neural network to infer advective fields based on satellite imagery

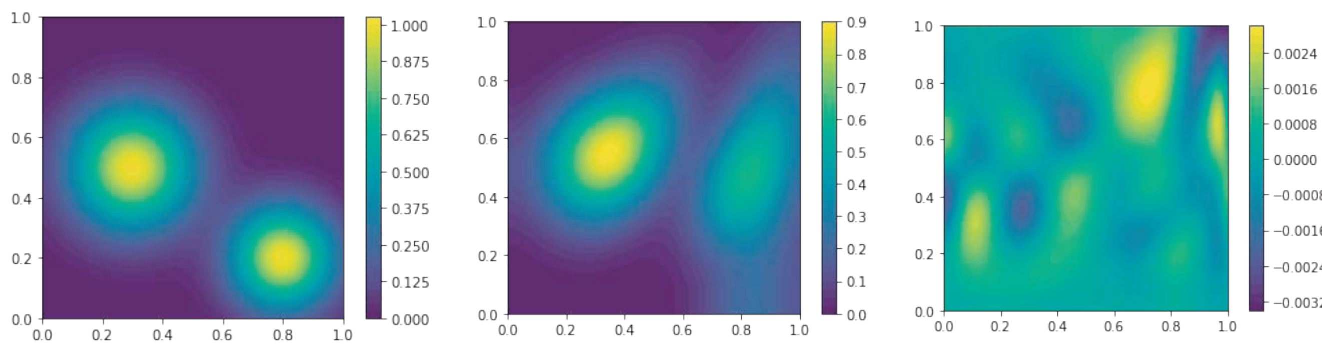

initital test concentation **predicted concentation** **error**

Filling the polar data gap with partial differential equations

hole in satellite coverage of sea ice concentration field

previously assumed ice covered

Gap radius: 611 km
06 January 1985

Gap radius: 311 km
30 August 2007

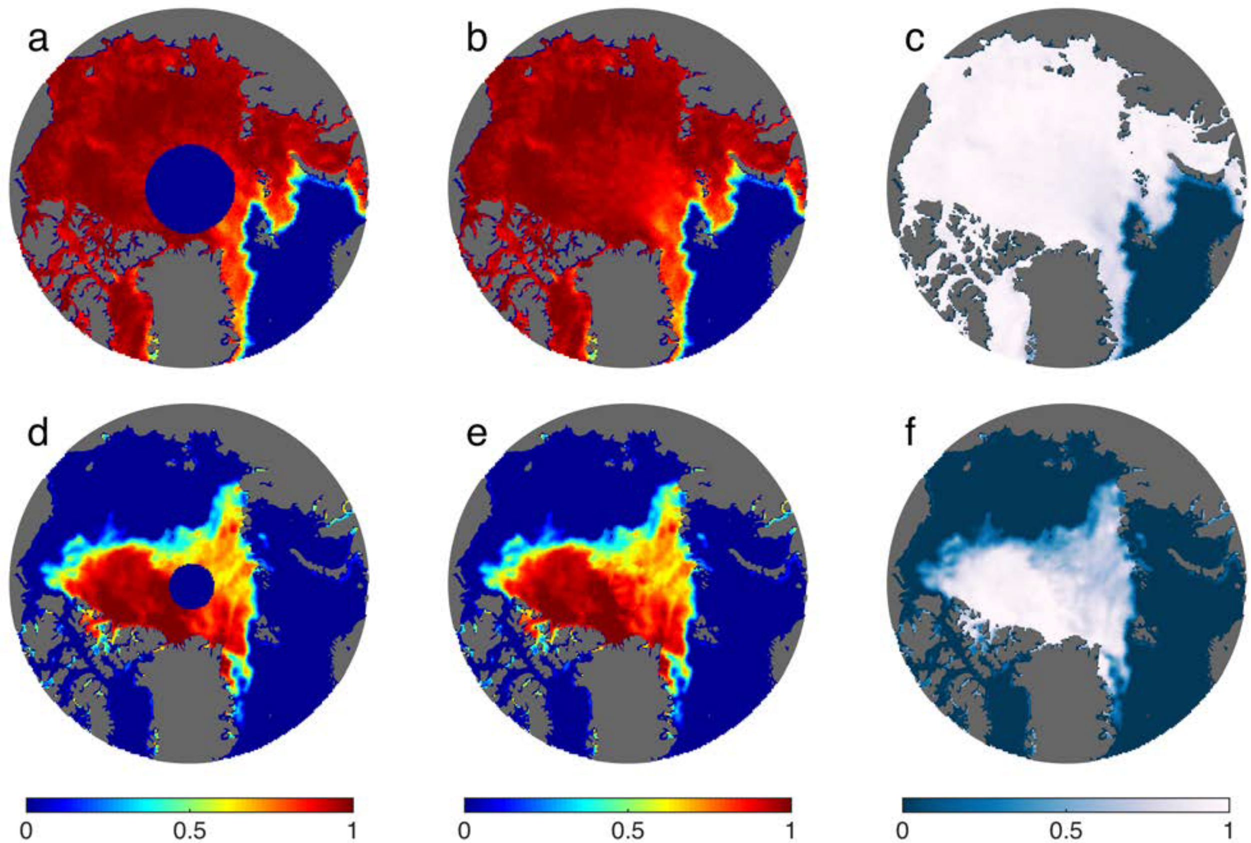

$$\Delta\psi=0$$

fill = harmonic function with learned stochastic term

Strong and Golden, *Remote Sensing* 2016
Strong and Golden, *SIAM News* 2017

NOAA/NSIDC Sea Ice Concentration CDR product update will use our PDE method.

www.math.utah.edu/~golden

www.math.utah.edu/~golden/resources/grad2022

two PDFs on sea ice physics and biology
3 minute movie on Antarctic expedition
opening video from Frontiers of Science
NAMS overview on sea ice modeling 2020

University of Utah Sea Ice Modeling Group (2017-2021)

Senior Personnel: Ken Golden, Distinguished Professor of Mathematics
Elena Cherkaev, Professor of Mathematics
Court Strong, Associate Professor of Atmospheric Sciences
Ben Murphy, Adjunct Assistant Professor of Mathematics

Postdoctoral Researchers: Noa Kraitzman (now at ANU), Jody Reimer - **sea ice ecology**

Graduate Students: Kyle Steffen (now at UT Austin with Clint Dawson)
Christian Sampson (now at UNC Chapel Hill with Chris Jones)
Huy Dinh (now a sea ice MURI Postdoc at NYU/Courant)
Rebecca Hardenbrook
David Morison (Physics Department)
Ryleigh Moore
Delaney Mosier
Daniel Hallman

Undergraduate Students: Kenzie McLean, Jacqueline Cinella Rich,
Dane Gollero, Samir Suthar, Anna Hyde, Kitsel Lusted,
Ruby Bowers, Kimball Johnston, Jerry Zhang,
Nash Ward, David Gluckman, Nicole Forrester, ...

High School Students: Titus Quah, Dylan Webb, Powell Holzner, Elias Sigman, ...

ISSN 0002-9920 (print)
ISSN 1088-9477 (online)

Notices

of the American Mathematical Society

November 2020

Volume 67, Number 10

AMERICAN MATHEMATICAL SOCIETY

Advancing research. Creating connections.

The cover is based on "Modeling Sea Ice," page 1535.

Buchanan Bay, Antarctica   Mertz Glacier Polynya Experiment   July 1999

Conclusions

1. Sea ice is a fascinating multiscale composite with structure similar to many other natural and man-made materials.

2. Mathematical methods developed for sea ice advance the theory of composites and other areas of science and engineering.

3. Homogenization and statistical physics help ***link scales in sea ice and composites***; provide rigorous methods for finding effective behavior; advance sea ice representations in climate models.

4. Fluid flow through sea ice mediates melt pond evolution and many processes important to climate change and polar ecosystems.

5. Field experiments are essential to developing relevant mathematics.

6. Our research is helping to improve projections of climate change, the fate of Earth's sea ice packs, and the ecosystems they support.

Modeling Sea Ice

Kenneth M. Golden, Luke G. Bennetts, Elena Cherkaev, Ian Eisenman, Daniel Feltham, Christopher Horvat, Elizabeth Hunke, Christopher Jones, Donald K. Perovich, Pedro Ponte-Castañeda, Courtenay Strong, Deborah Sulsky, and Andrew J. Wells

Kenneth M. Golden is a Distinguished Professor of Mathematics at the University of Utah. His email address is golden@math.utah.edu.

Luke G. Bennetts is an associate professor of applied mathematics at the University of Adelaide. His email address is luke.bennetts@adelaide.edu.au.

Elena Cherkaev is a professor of mathematics at the University of Utah. Her email address is elena@math.utah.edu.

Ian Eisenman is an associate professor of climate, atmospheric science, and physical oceanography at the Scripps Institution of Oceanography at the University of California San Diego. His email address is eisenman@ucsd.edu.

Daniel Feltham is a professor of climate physics at the University of Reading. His email address is d.l.feltham@reading.ac.uk.

Christopher Horvat is a NOAA Climate and Global Change Postdoctoral Fellow at the Institute at Brown for Environment and Society at Brown University. His email address is christopher_horvat@brown.edu.

Elizabeth Hunke is a deputy group leader, T-3 fluid dynamics and solid mechanics group at the Los Alamos National Laboratory. Her email address is eclare@lanl.gov.

Christopher Jones is a Bill Guthridge Distinguished Professor of Mathematics at the University of North Carolina, Chapel Hill. His email address is ckrtj@unc.edu.

Donald K. Perovich is a professor of engineering at the Thayer School of Engineering at Dartmouth College. His email address is donald.k.perovich@dartmouth.edu.

Pedro Ponte-Castañeda is a Raymond S. Markowitz Faculty Fellow and professor of mechanical engineering and applied mechanics and of mathematics at the University of Pennsylvania. His email address is ponte@seas.upenn.edu.

Courtenay Strong is an associate professor of atmospheric sciences at the University of Utah. His email address is court.strong@utah.edu.

Deborah Sulsky is a professor of mathematics and statistics and of mechanical engineering at the University of New Mexico. Her email address is sulsky@math.unm.edu.

Andrew J. Wells is an associate professor of physical climate science at the University of Oxford. His email address is Andrew.Wells@physics.ox.ac.uk.

Communicated by Notices *Associate Editor Reza Malek-Madani.*

For permission to reprint this article, please contact: reprint-permission@ams.org.

Ising Model for a Ferromagnet

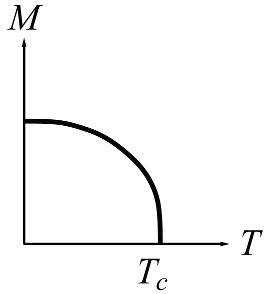

Curie point
critical temperature

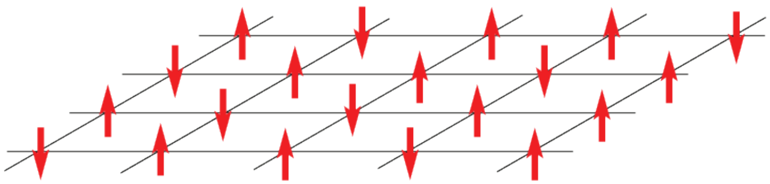

applied magnetic field H

$$s_i = \begin{cases} +1 & \text{spin up} \\ -1 & \text{spin down} \end{cases}$$

blue

white

$$\mathcal{H} = -H \sum_i s_i - J \sum_{<i,j>} s_i s_j$$

nearest neighbor Ising Hamiltonian

islands of like spins

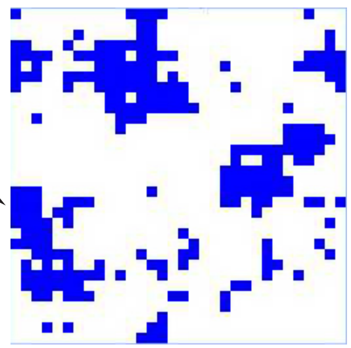

$$M(T,H) = \lim_{N\to\infty} \frac{1}{N} \left\langle \sum_j s_j \right\rangle$$

effective magnetization

energy is lowered when nearby spins align with each other, forming **magnetic domains**

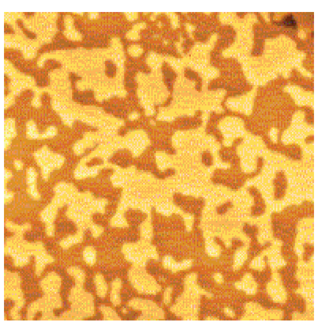

magnetic domains in cobalt

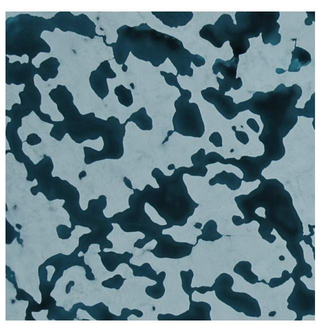

melt ponds (Perovich)

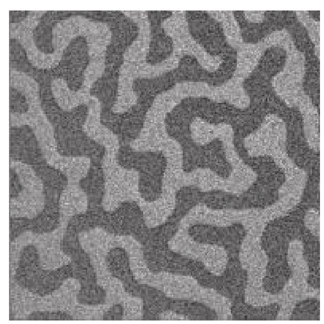

magnetic domains in cobalt-iron-boron

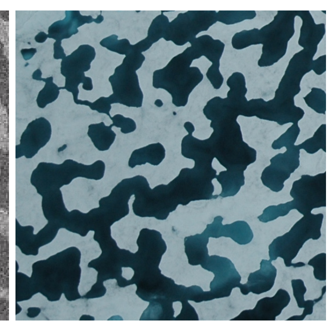

melt ponds (Perovich)

What is our research about?

Inputs, Ingredients

COMPOSITE MATERIALS

electrical engineering,
stealth technology

porous media,
oil extraction

statistical mechanics
of ferromagnets

Anderson localization,
semiconductor physics

random matrix theory

differential equations

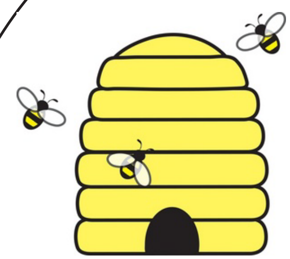

cross pollination

magnets
radar absorbers
human bone
rat brains

MODELING SEA ICE

Outputs, Impacts

CLIMATE MODELING

sea ice physics
& biology

composites,
polycrystals

remote sensing

advection diffusion

biomedical imaging,
biomaterials, EPS

polar microbial ecology

Modeling sea ice drives advances in many areas of science and engineering.

percolation theory

probabilistic theory of connectedness

impermeable　　　　　　　　　　permeable

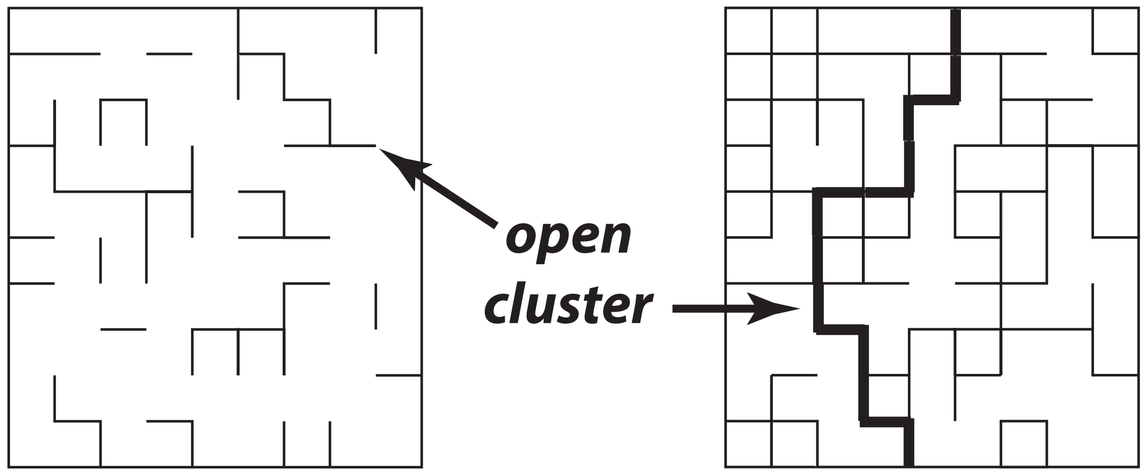

$p = 1/3$　　　　　　　　　　$p = 2/3$

$$\textit{bond} \longrightarrow \begin{cases} \textbf{open} & \text{with probability } p \\ \textbf{closed} & \text{with probability } 1-p \end{cases}$$

percolation threshold

$$p_c = 1/2 \quad \text{for} \quad d = 2$$

smallest *p* for which there is an infinite open cluster

Newsjournal of the Society for Industrial and Applied Mathematics
sinews.siam.org

siam news

Volume 53/ Issue 9
November 2020

Special Issue on the Mathematics of Planet Earth

*Read about the application of mathematics and computational science to issues concerning invasive populations, Arctic sea ice, insect flight, and more in this Planet Earth **special issue**!*

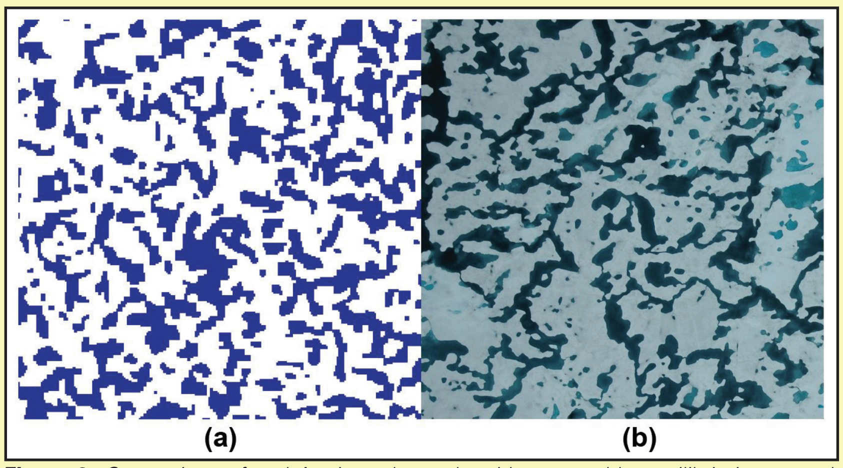

Figure 3. *Comparison of real Arctic melt ponds with metastable equilibria in our melt pond Ising model.* **3a.** *Ising model simulation.* **3b.** *Real melt pond photo. Figure 3a courtesy of Yiping Ma, 3b courtesy of Donald Perovich.*

Vast labyrinthine ponds on the surface of melting Arctic sea ice are key players in the polar climate system and upper ocean ecology. Researchers have adapted the Ising model, which was originally developed to understand magnetic materials, to study the geometry of meltwater's distribution over the sea ice surface. In an article on page 5, Kenneth Golden, Yiping Ma, Courtenay Strong, and Ivan Sudakov explore model predictions.

Controlling Invasive Populations in Rivers

By Yu Jin and Suzanne Lenhart

Flow regimes can change significantly over time and space and strongly impact all levels of river biodiversity, from the individual to the ecosystem. Invasive species in rivers—such as bighead and silver carp, as well as quagga and zebra mussels—continue to cause damage. Management of these species may include targeted adjustment of flow rates in rivers, based on recent research that examines the effects of river morphology and water flow on rivers' ecological statuses. While many previous methodologies rely on habitat suitability models or oversimplification of the hydrodynamics, few studies have focused on the integration of ecological dynamics into water flow assessments.

Earlier work yielded a hybrid modeling approach that directly links river hydrology with stream population models [3]. The hybrid model's hydrodynamic component is based on the water depth in a gradually varying river structure. The model derives the steady advective flow from this structure and relates it to flow features like water discharge, depth, velocity, cross-sectional area, bottom roughness, bottom slope, and gravitational acceleration. This approach facilitates both theoretical understanding and the generation of quantitative predictions, thus providing a way for scientists to analyze the effects of river fluctuations on population processes.

When a population spreads longitudinally in a one-dimensional (1D) river with spatial heterogeneities in habitat and temporal fluctuations in discharge, the resulting hydrodynamic population model is

$$
\begin{aligned}
N_t = -A_t(x,t)\frac{N}{A(x,t)} &+ \\
\frac{1}{A(x,t)}\Big(D(x,t)A(x,t)N_x\Big)_x &- \\
\frac{Q(t)}{A(x,t)}N_x + rN\left(1-\frac{N}{K}\right)&
\end{aligned}
$$

$$
\begin{aligned}
&N(0,t)=0 && \text{on } (0,T), x=0,\\
&N_x(L,t)=0 && \text{on } (0,T), x=L,\\
&N(x,0)=N_0(x) && \text{on } (0,L), t=0
\end{aligned}
\qquad (1)
$$

See **Invasive Populations** *on page 4*

Modeling Resource Demands and Constraints for COVID-19 Intervention Strategies

By Erin C.S. Acquesta, Walt Beyeler, Pat Finley, Katherine Klise, Monear Makvandi, and Emma Stanislawski

As the world desperately attempts to control the spread of COVID-19, the need for a model that accounts for realistic trade-offs between time, resources, and corresponding epidemiological implications is apparent. Some early mathematical models of the outbreak compared trade-offs for non-pharmaceutical interventions [3], while others derived the necessary level of test coverage for case-based interventions [4] and demonstrated the value of prioritized testing for close contacts [7].

Isolated analyses provide valuable insights, but real-world intervention strategies are interconnected. Contact tracing is the lynchpin of infection control [6] and forms the basis of prioritized testing. Therefore, quantifying the effectiveness of contact tracing is crucial to understanding the real-life implications of disease control strategies.

Contact Tracing Demands

Contact tracers are skilled, culturally competent interviewers who apply their knowledge of disease and risk factors when notifying people who have come into contact with COVID-19-infected individuals. They also continue to monitor the situation after case investigations [1].

Case investigation consists of four steps:

1. Identify and notify cases
2. Interview cases
3. Locate and notify contacts
4. Monitor contacts.

Most health departments are implementing case investigation, contact identification, and quarantine to disrupt COVID-19 transmission. The timeliness of contact tracing is constrained by the length of the infectious period, the turn-around time for testing and result reporting, and the ability to successfully reach and interview patients and their contacts. The European Centre for Disease Prevention and Control approximates that contact tracers spend one to two hours conducting an interview [2]. Estimates regarding the timelines of other steps are limited to subject matter expert elicitation and can vary based on cases' access to phone service or willingness to participate in interviews.

Bounded Exponential

The fundamental structure of our model follows traditional susceptible-exposed-infected-recovered (SEIR) compartmental modeling [5]. We add an asymptomatic population A, a hospitalized population H, and disease-related deaths D, as well as corresponding quarantine states. We define the states $\{S_i, E_i, A_i, I_i, H, R, D\}_{i=0,1}$ for our compartments, such that $i=0$ and $i=1$ correspond to unquarantined and quarantined respectively. Rather than focus on the dynamics that are associated with the state transition diagram in Figure 1, we introduce a formulation for the real-time demands on contact tracers' time as a function of infection prevalence, while also respecting constraints on resources.

When the work that is required to investigate new cases and monitor existing contacts exceeds available resources, a backlog develops. To simulate this backlog, we introduce a new compartment C for tracking the dynamic states of cases:

$$\frac{dC}{dt} = [flow_{in}] - [flow_{out}].$$

Flow into the backlog compartment, represented by $[flow_{in}]$, reflects case identification that is associated with the following transitions in the model:

– The rate of random testing: $q_{rA}(t)A_0(t) \rightarrow A_1(t)$ and $q_{rI}(t)I_0(t) \rightarrow I_1(t)$

– Testing triggered by contact tracing: $q_{tA}(t)A_0(t) \rightarrow A_1(t)$, $q_{tI}(t)I_0(t) \rightarrow I_1(t)$, and $q_{tE}(t)E_1(t) \rightarrow \{A_1(t), I_1(t)\}$

– The population that was missed by the non-pharmaceutical interventions that require hospitalization: $\tau_{IH}(t)I_0(t) \rightarrow H(t)$.

Here, $q_{r*}(t)$ defines the time-dependent rate of random testing, $q_{t*}(t)$ signifies the time-dependent rate of testing that is triggered by contact tracing, and τ_{IH} is the inverse of the expected amount of time for which an infected individual is symptomatic before hospitalization. These terms collectively provide the simulated number of newly-identified positive COVID-19 cases. However, we also need the average number of contacts per case. We thus define function $\mathcal{K}(\kappa, T_S, \phi_\kappa)$ that depends on the average number of contacts a day (κ), the average number of days for which an individual is infectious before going into isolation (T_S), and the likelihood that the individual

See **COVID-19 Intervention** *on page 3*

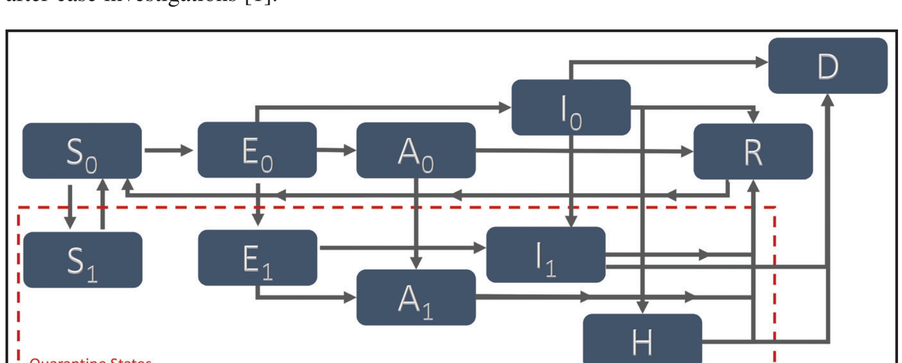

Figure 1. *Disease state diagram for the compartmental infectious disease model. Figure courtesy of the authors.*

Nonprofit Org
U.S. Postage
PAID
Permit No 360
Bellmawr, NJ

SOCIETY for INDUSTRIAL and APPLIED MATHEMATICS
3600 Market Street, 6th Floor
Philadelphia, PA 19104-2688 USA

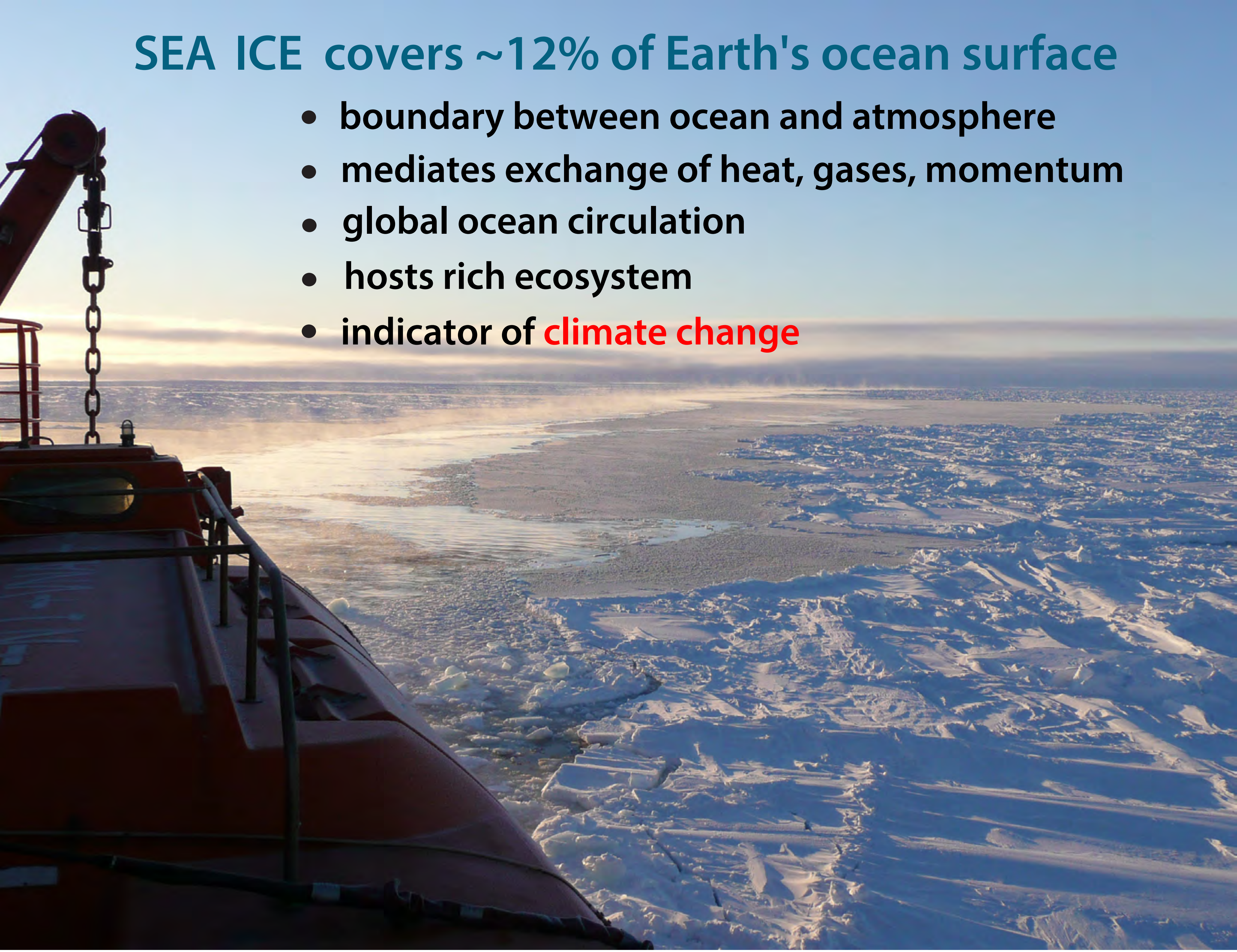
SEA ICE covers ~12% of Earth's ocean surface
• boundary between ocean and atmosphere
• mediates exchange of heat, gases, momentum
• global ocean circulation
• hosts rich ecosystem
• indicator of climate change

polar ice caps critical to global climate in reflecting incoming solar radiation

white snow and ice reflect

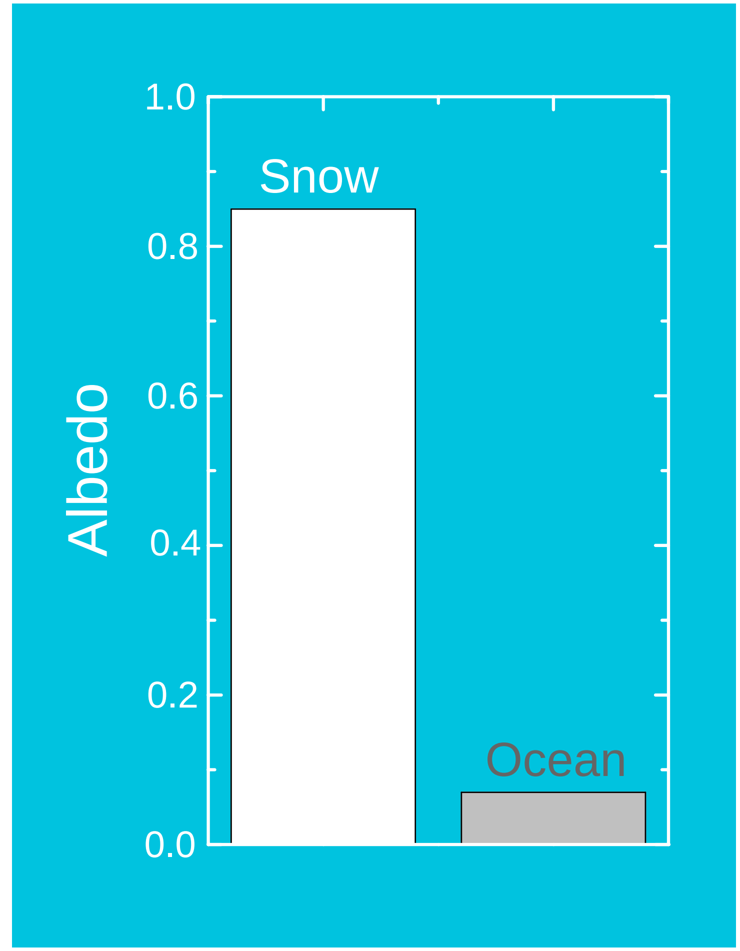

dark water and land absorb

$$\textbf{\textit{albedo}}\ \alpha = \frac{\text{reflected sunlight}}{\text{incident sunlight}}$$

challenge:

Represent sea ice more realistically in climate models to improve projections.

How do patterns of dark and light evolve?

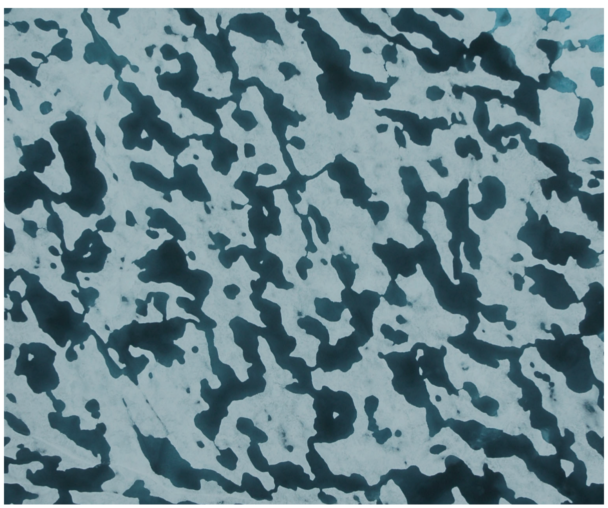

Account for key processes

e.g. melt pond evolution

Including PONDS in simulations LOWERS predicted sea ice volume over time by 40%.

Flocco, Schroeder, Feltham, Hunke, *JGR Oceans* 2012

... and other sub-grid scale structures and processes.

linkage of scales

Algal bloom model

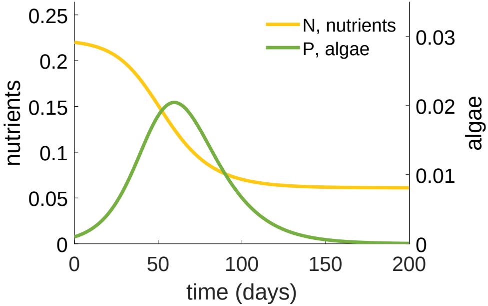

- poor agreement with data
- poor agreement between models

Steinacher, M., et al. (2010). *Biogeosciences*, 7(3), 979-1005

How do we analyze this model?

Monte Carlo simulations?

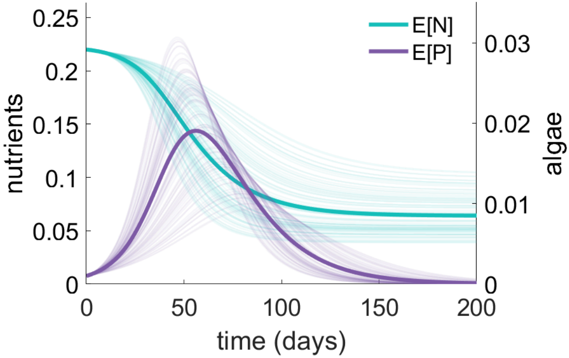

Too slow! Full algae model takes **8 hours** (cloud computing).

Polynomial chaos expansions

$$N(t;B,P_0,N_0) \approx N_V(t;B,P_0,N_0) := \sum_{j=1}^{n} \widetilde{N}_j(t)\phi_j(B,P_0,N_0),$$

$$P(t;B,P_0,N_0) \approx P_V(t;B,P_0,N_0) := \sum_{j=1}^{n} \widetilde{P}_j(t)\phi_j(B,P_0,N_0),$$

where

- $V := \mathrm{span}\{\phi_j\}_{j=1}^{n}$
- ϕ_j are orthogonal polynomials that form a basis for V
- $(\widetilde{N}_j, \widetilde{P}_j)$ need to be computed

Xiu, D. (2010). Numerical methods for stochastic computations. Princeton university press.